Response to reviewer' comments

On the manuscript **nhess-2020-132**

revised for publication in

NHESS

We wish to thank the reviewer for their valuable suggestions. We agree with most of the critiques raised during the review process, and we did our best to incorporate them in the revised paper.

Considering the reviewers' suggestions, we deeply modified the introduction and the discussion of the paper. New figures have been added to discuss further the validation of the proposed models [i.e. Fig. 5 in the revised manuscript], and some figures and their captions have been modified to improve clarity. We also combined the information of tables 4 and 5 to a new table (now table 3). We added a new discussion on the correlation between differences with FEMA extents, and the provided simulations (Also added in table 4, in the current submission), and we re-structured the discussion and the conclusion.

Here is a detailed response [in italics] to each point raised during the review [underlined font].

Response to reviewer #1:

<u>1. The literature review for frequency-based effect estimate of compound-event flooding (Line 69-76) is obscure. What is the missing link in the current research and why most of the studies failed to or avoided to explore the frequency and risk assessment of the compound flooding? It seems in this study the authors designed several compound scenarios to consider the probability of precipitation and surge as a solution to the shortcoming associated with compound flood risk assessment. If this is the case, more details on the related theories and methodologies should be presented in the introduction.</u>

We thank the reviewer for this comment. We modified the introduction to provide a better framework for this study and highlighted the importance of this work. We improved the literature background to highlight more clearly what is missing in current research, and what this work is addressing. We rephrased and reorganized the introduction. Some key changes are as follows:

Line 36- 39: Concurrent with the rise in event intensities, the elevated damage, and disruption caused by compound flooding (CF) to critical infrastructure (CI) and services, including electrical systems, water, and sewage treatment facilities, and other utilities that underpin modern society, have substantial adverse socioeconomic impacts, especially in low-lying coastal areas, where almost 40 percent of people in the United States live (NOAA, 2013).

Line 45- 54: Recent studies have underlined the importance of understanding and quantifying the flood impacts on critical infrastructure, and their broader implications in risk management and catchment-level planning (Chang et al., 2007; McEvoy et al., 2012; Ziervogel et al., 2014; de Bruijn et al., 2019; Pearson et al., 2018; Pant et al., 2018; Dawson, 2018). Some authors have estimated the frequency of compound flooding and provide approaches to risk assessment based on the joint probability of precipitation and surge (Bevacqua et al., 2019; Wahl et al., 2015). The spatial extent and depth of compound flooding can vary in frequency (Quinn, et al., 2019) if any of the components of CF is not taken into consideration while evaluating flood frequency. Both storm surges and heavy precipitation, and their interplay, are likely to change in the future (Field et al., 2012, Dottori et al., 2018; Blöschl et al., 2017; Muis et al., 2016; Marsooli et al., 2019; Vousdoukas et al., 2018). Nonetheless, the effects of CF, considering the climate change impact, have not been thoroughly explored yet.

Line 56- 69: We present a hydrologic-hydrodynamic modeling framework to evaluate the integrated impact of flood drivers causing CF by synthesizing current and future scenarios. This study enables the quantitative measurement of CF hazard cast on critical infrastructures in terms of flood depth and flood extent by *observing actual storm-induced floods and drawing information from synthetic scenarios. To project the combined flood hazard in future climate conditions, we integrated the effects of SLR, tides, and synthetic hurricane event simulations into the flood hazard exposure.*

Even though past research on the assessment of damages to the power system components or other related infrastructures has proposed design and operation countermeasures and remedies (i.e. Kwasinski et al. 2009; Reed et al. 2010; Abi-Sarma and Henry, 2011; Chang et al., 2007; de Bruijn et al., 2019; Pearson et al., 2018; Pant et al., 2018; Dawson, 2018), these studies lack a comprehensive hazard assessment on power grid components, and.potential changes due to climate change.

2. In section 2.3, it is better to use a table to describe these compound scenarios and their related hurricanes, SLR, tide conditions, and other attributes.

We thank the reviewer for this comment. We combined the information of tables 4 and 5 to table 3 in the submitted manuscript. We have rephrased section 2.3 accordingly.

3. In section 2.4, which site does Figure 5 present for? The red rectangle shows a window of 48 hrs, not 24 hrs. What criterion is used for selecting the window size?

We thank the reviewer for this comment. The rectangle was simply to bring attention to the peak and highlight the changes in depth for the different scenarios. We have removed the rectangle from the figure and clarified more in the text. The figure number is now "Figure 6". The site information is added to the caption of the figure.

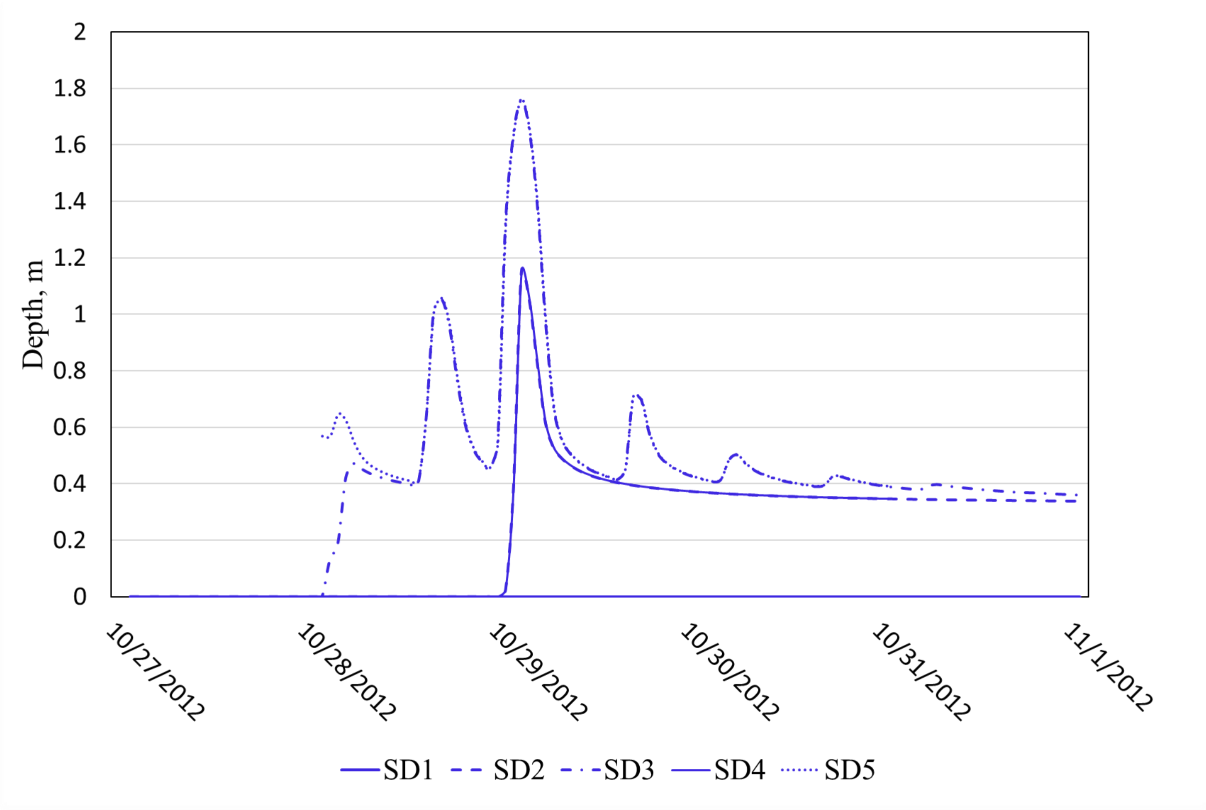

Figure 6: Example of time series of depth values for the different scenarios of Sandy event at CI3 [SD1 to SD5, readers should refer to Table 3 and chapter 2.4 for specification on the scenarios]

4. In Lines such as 230, 237, Table 4 should be Table 5.

We thank the reviewer for this comment. We have fixed the text according to the modified table and figure numbers.

5. Figure 8 shows the inundated period for each site; however, it cannot be seen that any data show 20% or 90% for SD1 or SD5 in the subgraphs of CI7 and CI8.

We thank the reviewer for this comment. We clarified section 3.3. More in detail, we added the following paragraph.

line 368-371: ……. If a critical infrastructure shows 0%, it means that for that scenario/event the water didn't reach the substation at all, at least during the simulated timeframe. This could be due to the water flooding other upstream locations, and therefore draining away from the station, or because the topography of the landscape actually prevented water from reaching the area for some specific events.

6. The section of concluding remarks should be enhanced. The current conclusions are not intensive enough to show the findings of this paper. At least some quantitative analysis can be summarized and presented for readers to better understand how this work promotes the current risk assessments of compound flood hazards.

We thank the reviewer for this comment. We rephrased the concluding remarks as per the reviewer's suggestion.

7. There are some mistakes in grammar and spelling and the authors also did not pay enough attention to punctuation, which makes this manuscript more like a draft.

We thank the reviewer for their valuable suggestion. We proofread for grammar, spellings, and punctuations for better quality and readability.

References

A. K*wasinski, W.W. Weaver, P.L. Chapman and P.T. Krein, "Telecommunications Power Plant Damage Assessment for Hurricane Katrina – Site Survey and Follow-Up Results," IEEE Systems Journal, vol. 3, no. 3, pp. 277–287, Nov. 2009.*

B. D.A. Reed, M.D. Powell and J.M. Westerman, "Energy Supply System Performance for Hurricane Katrina," Journal of Energy Engineering, pp. 95–102, Dec. 2010.

C. N. Abi-Samra and W. Henry, "Actions Before and After a Flood – Substation Protection and Recovery from Weather Related Water Damage," IEEE Power & Energy Magazine, pp. 52–58, Mar/Apr. 2011.

D. Chang, S. E., McDaniels, T. L., Mikawoz, J., & Peterson, K.: Infrastructure failure interdependencies in extreme events: power outage consequences in the 1998 Ice Storm. Natural Hazards, 41(2), 337–358. https://doi.org/10.1007/s11069-006-9039-4, 2007.

E. Dawson, R. J., Thompson, D., Johns, D., Wood, R., Darch, G., Chapman, L., Hughes, P. N., Watson, G. V. R., Paulson, K., Bell, S., Gosling, S. N., Powrie, W. and Hall, J. W.: A systems framework for national assessment of climate risks to infrastructure, Philos. Trans. R. Soc. A Math. Phys. Eng. Sci., 376(2121), doi:10.1098/rsta.2017.0298, 2018.

F. de Bruijn, K. M., Maran, C., Zygnerski, M., Jurado, J., Burzel, A., Jeuken, C. and Obeysekera, J.: Flood resilience of critical infrastructure: Approach and method applied to Fort Lauderdale, Florida, Water (Switzerland), 11(3), doi:10.3390/w11030517, 2019.

G. Pant, R., Thacker, S., Hall, J. W., Alderson, D. and Barr, S.: Critical infrastructure impact assessment due to flood exposure, J. Flood Risk Manag., 11(1), 22–33, doi:10.1111/jfr3.12288, 2018.

H. Pearson, J., Punzo, G., Mayfield, M., Brighty, G., Parsons, A., Collins, P., Jeavons, S. and Tagg, A.: Flood resilience: consolidating knowledge between and within critical infrastructure sectors, Environ. Syst. Decis., 38(3), 318–329, doi:10.1007/s10669-018-9709-2, 2018.

Response to reviewer #2:

Major points

1. The title is awkward to read. I suggest something as "Flood impact on coastal critical infrastructures considering compound flood events in current and future climate".

We thank the reviewer for this suggestion. We changed the title to "Impact of Compound Flood Event on Coastal Critical Infrastructures Considering Current and Future Climate".

2. The Introduction is quite general and not specific enough. What the Author describes as a "a dynamic framework to project the combined hazard" is nothing else that a hydrological model and a hydrodynamic model run in cascade and forced with both actual and synthetic data.

We thank the reviewer for this comment. We modified the introduction to provide a better framework for this study and highlighted the importance of this work. We improved the literature background to highlight more clearly what is missing in current research, and what this work is addressing. We rephrased and reorganized the introduction. Some key changes are as follows:

Line 36- 39: Concurrent with the rise in event intensities, the elevated damage, and disruption caused by compound flooding (CF) to critical infrastructure (CI) and services, including electrical systems, water, and sewage treatment facilities, and other utilities that underpin modern society, have substantial adverse socioeconomic impacts, especially in low-lying coastal areas, where almost 40 percent of people in the United States live (NOAA, 2013).

Line 45- 54: Recent studies have underlined the importance of understanding and quantifying the flood impacts on critical infrastructure, and their broader implications in risk management and catchment-level planning (Chang et al., 2007; McEvoy et al., 2012; Ziervogel et al., 2014; de Bruijn et al., 2019; Pearson et al., 2018; Pant et al., 2018; Dawson, 2018). Some authors have estimated the frequency of compound flooding and provide approaches to risk assessment based on the joint probability of precipitation and surge (Bevacqua et al., 2019; Wahl et al., 2015). The spatial extent and depth of compound flooding can vary in frequency (Quinn, et al., 2019) if any of the components of CF is not taken into consideration while evaluating flood frequency. Both storm surges and heavy precipitation, and their interplay, are likely to change in the future (Field et al., 2012, Dottori et al., 2018; Blöschl et al., 2017; Muis et al., 2016; Marsooli et al., 2019; Vousdoukas et al., 2018). Nonetheless, the effects of CF, considering the climate change impact, have not been thoroughly explored yet.

Line 56- 69: We present a hydrologic-hydrodynamic modeling framework to evaluate the integrated impact of flood drivers causing CF by synthesizing current and future scenarios. This study enables the quantitative measurement of CF hazard cast on critical infrastructures in terms of flood depth and flood extent by observing actual storm-induced floods and drawing information from synthetic scenarios. To project the combined flood hazard in future climate conditions, we integrated the effects of SLR, tides, and synthetic hurricane event simulations into the flood hazard exposure.

Even though past research on the assessment of damages to the power system components or other related infrastructures has proposed design and operation countermeasures and remedies (i.e. Kwasinski et al. 2009; Reed et al. 2010; Abi-Sarma and Henry, 2011; Chang et al., 2007; de Bruijn et al., 2019; Pearson et al., 2018; Pant et al., 2018; Dawson, 2018), these studies lack a comprehensive hazard assessment on power grid components, and.potential changes due to climate change.

a. Nonetheless, an estimation of the expected frequency is fundamental when treating compound events. This aspect is quite lacking in the paper.

We thank the reviewer for this comment. We definitely agree that a frequency estimation is critical in treating compound events. This, however, goes beyond the scope of the current manuscript. For this work, we aimed to set up a modeling framework, and use it to demonstrate the importance of compound events on infrastructure flooding based on past hurricane events and synthetic hurricane cases simulated in future climate conditions. In the discussion we have stated our intention for future works with the following text:

Line 449- 454: Future research should consider improved estimation methods, including more detailed information on the variability of river properties (i.e. depth and width). Future works should also relate the frequency of inundation depths to return periods of precipitation, river flows, and surges, as well as differentiate among the individual effects of the components to determine the role of each in flooding impact. This can be a very useful piece of information for deciding whether and where to take measures in terms of flood occurrence and the potential relocation of CI to avoid catastrophic compound flood events.

Many statements are quite imprecise. For example, it is stated that the focus is on coastal power grid substations, but this is not correct.

We thank the reviewer for this comment. We have added the following text to address this comment:

Line 89- 91: Among the case study sites, two CIs are relatively inland [CI3 and CI4] (table 1: see hydrologic distance. Figure 1: see coastal boundary), nonetheless all the sites are included within the Coastal Area as defined by Connecticut General Statute (CGS) 22a-94(a) [https://www.cga.ct.gov/current/pub/chap_444.htm#sec_22a-94].

We also included the boundary in Figure 1 (see below).

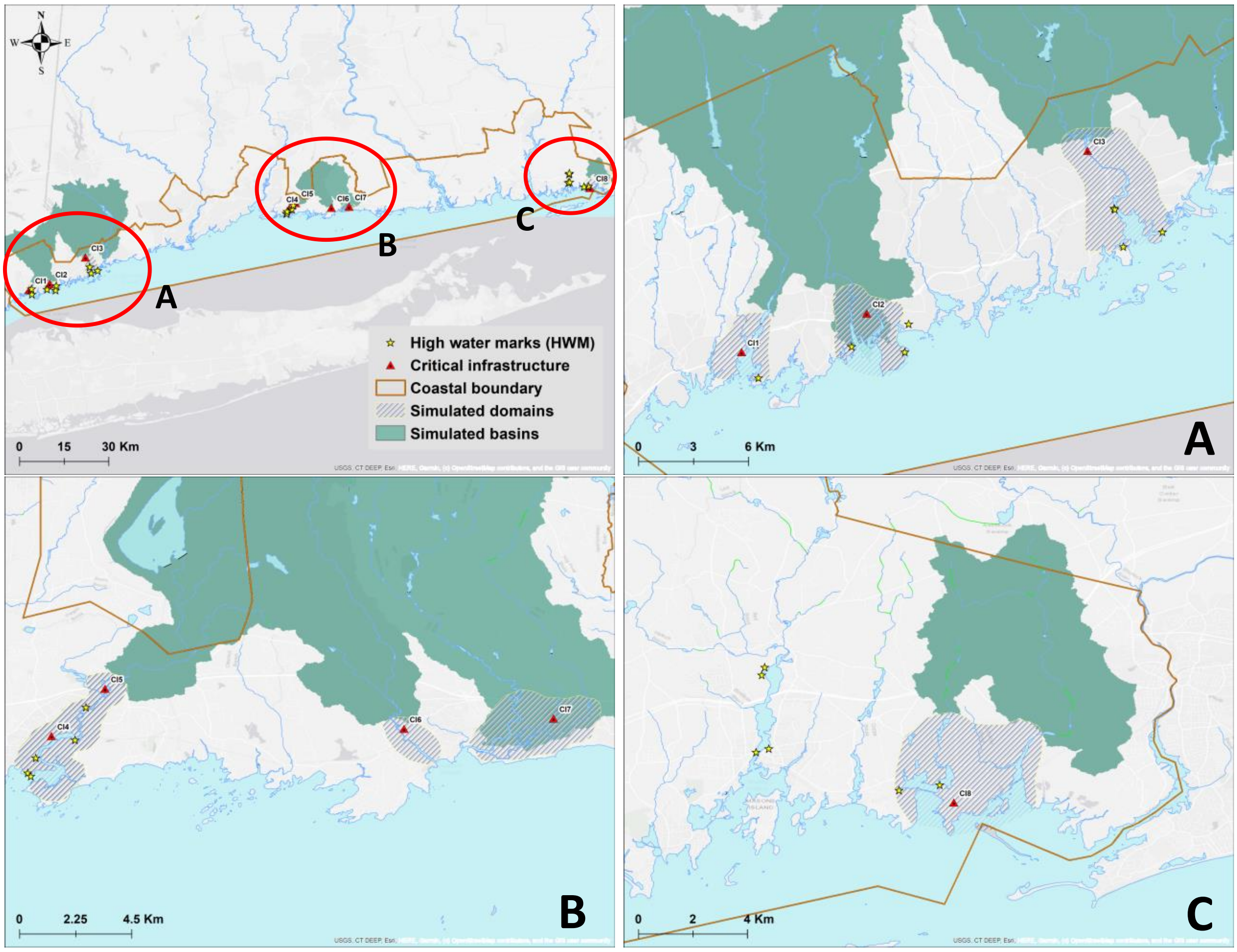

Figure 1: Study area with associated watersheds and simulation domains. Locations of substations and USGS high water marks are also shown. Red circles in the top left-hand panel, and marked with A, B, and C are highlighted in panels A to C respectively. Background map by ESRI web-services, provided by UConn/CTDEEP, Esri, Garmin, USGS, NGA, EPA, USDA, NPS

3. No information is given about the chance of malfunctioning of power grid substations due to flooding. Are these substations built up to tolerate a given water depth?

We thank the reviewer for this comment. Due to confidentiality, we cannot provide exact information related to the critical water level for each infrastructure. The presented water depths are indicative numbers, useful to provide a comparison between the various events. In section 2.4, lines 253-260, we discussed the threshold used for the analysis of the flood depth at each station.

4. The paper only deals with the water depths at eight locations in which power grid substations are present, which is quite another (preliminary) issue. Moreover, at the end of the Introduction, two main questions are reported. First, it is said that the present work forms the basis on which to address these two questions (which is correct), then it is said that these questions are investigated, which is incorrect.

We thank the reviewer for this comment. We would like to underline that indeed, the paper aims to characterize the risk for critical electric grid infrastructures, and this is why we analyzed the water depth at the selected locations. We, however, also investigated the water depths in the entire model domain, by presenting the CDFs, and comparing the water extent to the FEMA 100 year flood maps, which provides an overall hazard assessment of the studied compound events. In the revised manuscript we rephrase the questions in the introduction, to provide a clearer description of the focus of our study. The new questions are:

Line 70- 74: The scenario-based analysis of this study formed the basis on which to address two questions:

(1) What are the characteristics of the tropical storm-related inundation, considering the compound effect of riverine and coastal flooding coinciding or not with peak high tides

(2) Will future climate (including SLR and intensification of storms due to warmer sea surface temperatures) bring a significant increase in flood impact for the power-grid coastal infrastructures?

5. Model calibration/validation. I'm not an expert of meteorological models, so I'm not commenting on. But for what concerns hydrological and hydrodynamic models, I have substantial concerns.

a. As for the hydrological model, the use of information on land use, land cover, and imperviousness ratio does not imply that an overparameterized model (as all spatially explicit and hyper-resolution model are) provides reliable results. The fact that the model was successfully verified in river basins within Connecticut, where all the watersheds simulated in this study reside, does not assure the model reliability in different river basins. Indeed, it is common that different rivers in the same country show very different hydrological behaviours. Calibration and validation should have been performed for the rivers considered in this study, and for the actual events (Sandy and Irene) the outcome of the model should have been compared with some measured data (no measured data within all the modelled domain seems quite an unrealistic picture).

We thank the reviewer for this comment. We clarified the calibration and validation process using the following text:

Line 147- 151: CREST-SVAS was calibrated and validated for the whole Connecticut river basin [that contains all the investigated sites] with an NSCE of 0.63 (Shen and Anagnostou, 2017). We further validated the model considering hourly flows in two locations within the Housatonic River and Naugatuck River watersheds with *an NSCE of 0.69 (Hardesty et al., 2018). The quality measures indicate a satisfactory model performance at the watershed scale over the topographic region that collectively include our study sites.*

> b. It is simply unacceptable that a riverine model is set-up using LiDAR data also for the submerged channel beds. Bed elevations MUST be corrected using proper bathymetric data (multibeam, cross sections, etc.) to obtain reliable results. Contrarily to what the Authors stated, it cannot be concluded that neglecting submerged channel bed, which results in an underestimation of channel conveyance capacity, would lead to an overestimation of the flood extent. A channel with a lower capacity can also confine an inundated area, whereas a greater conveyance capacity can cause further flooding as well. Furthermore, the model is validated considering water depth only, and not flood extent.

We agree with the reviewer on the importance of bathymetry in flood inundation modeling.

As an example, the following paragraphs illustrate how the proposed model provides good simulations, even when compared to running the model accounting for bathymetry.

For this, we applied a Discharge Correction Technique (DCT) to the hydrologically simulated discharge. DCT is based on the assumption that a given flow discharge can be separated into two components: the bankfull discharge, below the assessed water surface, and the discharge exceeding the LiDAR discharge, above the assessed water surface. This technique is used commonly to assess the discharge of a compound channel and is also known as the horizontally divided channel method (Bradbrook et al. 2004). To evaluate the bankfull discharge, we considered regional curves (Ahearn, 2004). Fig R1 shows for hurricane Irene [actual event], a comparison between the CREST-simulated discharge, and the DCT one. The results of the simulation carried out as presented in the manuscript, VS the simulation corrected using the DCT for CI1 is shown in Fig R2.

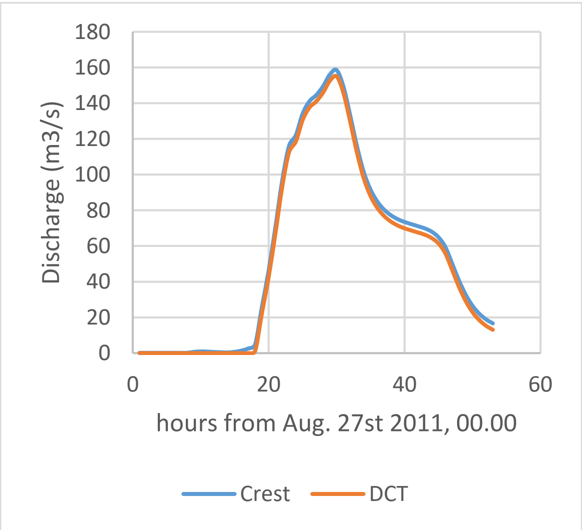

Figure R1: example of DCT as compared to CREST simulated discharge

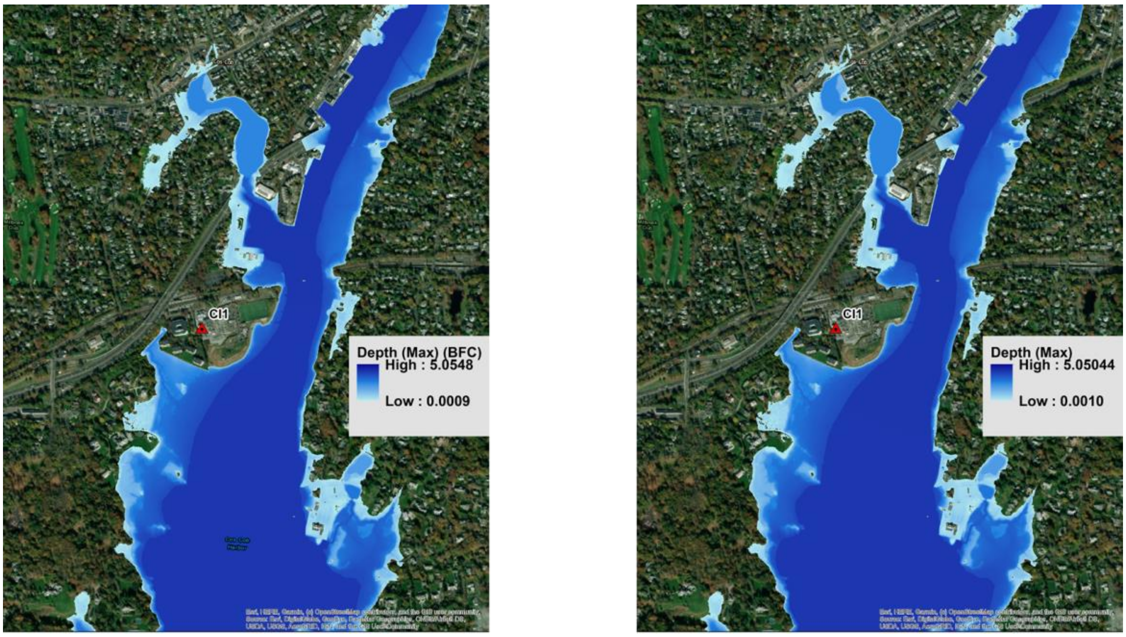

Figure R2: Maximum flood depth during the actual Irene event: left: streamflow with DCT, right: Streamflow without DCT, as presented in the submitted manuscript.

These results highlight how, for a larger event, where the floodplains are near fully flooded, the inclusion of bathymetry does not make substantial differences for the extent of flooding or the water depth. We did not include the above-explained analysis to the manuscript but based on the findings we added the following text to the revised manuscript:

Line 163- 169: The considered locations have no bathymetric (underwater topography) data represented in the DEM. In general, the impact of inclusion/exclusion of bathymetry data on the hydrodynamic model simulations will vary according to the river size and event severity (Cook & Merwade 2009). For the investigated events in this study, defence overflow and defence breaching mainly dominate flood risk. This means that we do not require detailed bathymetric information in the upstream main channel, thereby considerably simplifying the modeling problem (Bates et al. 2013). Therefore, we did not represent the flow of water in the main channel. Rather boundary conditions were given as time series of water surface elevation imposed along the defence crests.

Considering the reviewer comments, we included further clarification about the model validation, see our response to the below point

6. Figure 4 shows a comparison between modelled and measured water depth. Considering that two real flooding events (Sandy and Irene hurricanes) were simulated, I was expecting a comparison for these two events. Modelled water depths are reported in the figure using boxplot (instead of single values referring to these two real hurricane events), but it is not said from which set of simulations these boxplots are derived from.

We thank the reviewer for this comment. As validation data, we only have High water marks (HWM) and surge extent information for Sandy, not for Irene. Hence, we based our comparison on that event. We clarified the analysis with the following text:

Line 188- 191: An HWM does not necessarily indicate the maximum flood depth; rather, it can be a mark from a lower depth that lasts long enough to leave a trail. Based on this understanding, we compared the HWMs against the simulated flood depths within a 10x10m radius around the high water marks, also to avoid issues due to the presence of buildings in the DEM (Boxplots in Fig. 4).

Regarding the validation of the flood extent, we will provide further assessment in the revised manuscript. As for the water depth, the most accurate available information for flood extent is only available for Sandy.

Line 194- 199: Figure 5 shows a visual comparison for CI1 and CI2 between the simulated inundation (Fig.5 a, c), and the reference extent (Fig. 5 d,e). A slight overestimation of the flood level, ranging between 0.2 and 0.4 m, with a precision of 0.2 m or less, is observed for the inundation depths at the displayed locations, which is consistent with the results obtained locally, at the HWM locations (Fig. 4). Taking into consideration the accuracy of the inundation depth, the declared DEM accuracy (vertical RMSE ~0.3m), and the simplified modeling problem concerning bathymetry, the accuracy of the flood extent assessment was judged satisfactory.

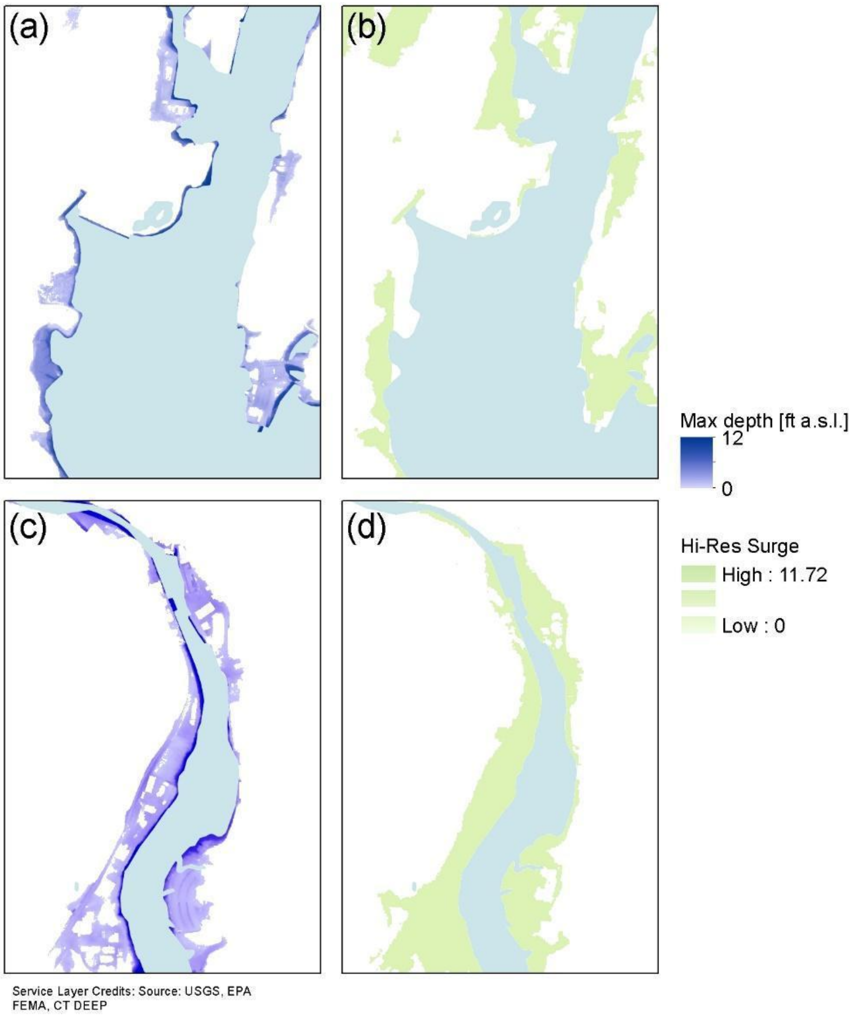

Figure 5: Comparison between the results of the proposed model for two selected locations (a,c, CI1, and CI2 respectively) and the maximum surge extent as proposed by CtEco (c,d respectively).

7. Finally, I agree with the comments raised by the Reviewer 2. In general, the manuscript should be substantially revised and arranged with far greater rigor.

We thank the reviewer for their valuable suggestion. We proofread for grammar, spellings, and punctuations for better quality and readability.

Minor points

• l. 55: "riverine models cannot capture the risk from tide-surge-SLR effects". In what a sense? While it is true that, traditionally, one looks at the river or at the coast one at a time, riverine models can naturally capture the risk induced by tidesurge-SLR on flooding in the form of higher free-surface elevations for tailwater effects, when forced with proper downstream boundary conditions. Moreover, if the riverine model includes floodable areas adjacent to the coast, the same hydrodynamic model can be used to assess coastal flooding too, it's only a matter of boundary conditions.

We thank the reviewer for this comment. We have removed this part of the text and rephrased most of the introduction. Please refer to the Chapter1: Introduction.

l. 56-57: Depending of what is meant for "riverine models", "the modelling of individual flood drivers separately mischaracterizes the true risk of flooding" is not a rigorous statement, as what the Authors affirms is true only when the effects of compound events are worsen than the sum of effects due to single forcing events

We thank the reviewer for this comment. We have removed this part of the text and rephrased most of the introduction. Please refer to the Chapter1: Introduction.

• l. 56: Barnard et al. 2017 is not present in the Bibliography.

We fixed the bibliography

• l. 73: "in frequency"? The sense of this sentence remains obscure to me.

We rephrased the sentence to -

Line 48- 49: Some authors have estimated the frequency of compound flooding and provide approaches to risk assessment based on the joint probability of precipitation and surge (Bevacqua et al., 2019; Wahl et al., 2015).

• l. 90: please repeat what kind of substations.

We used "power grid substations" instead of "substations"

• l. 109-111: I cannot recognize subsection a, b, and c in the text.

We have fixed them

• l. 157: extent of what? depth of what? (water, of course).

We rephrased it to "extent and the maximum depth of the flood" in the revised manuscript line 153

• l. 160: How were the building footprint used in the model? So many different approaches have been proposed. . .

We thank the reviewer for this comment. In the manuscript we explained more clearly how we approached this with the following text:

Line 157-162: The inundation maps are derived using a 1m LIDAR DEM (CtECO 2016) taken as base maps for the study reaches. To better represent the impacts of urban establishments on inundation dynamics, solid urban features such as houses and buildings, which obstruct the flow of stormwater, were added to the bare-earth DEM. For this, we considered the building footprints from (CtECO, 2012) and identified positions of buildings and houses in the DEM by increasing the elevation of the pixels within the building footprint polygons by an arbitrary height of 4.5 m, assuming one-story buildings.

• l. 279: Please explain how cumulative distribution function (CDF) of maximum flood depths were computed.

Line 244 252: To evaluate the flood hazard in terms of flood depth, we computed a Cumulative Distribution Function (CDF) to shows the probability that the flood depth will attain a value less than or equal to each measured value. We estimated the CDF using all the depth values of all the grid of the simulation domain, for the time step when the inundation was maximum. We evaluated the depth empirical exceedance probability (Hanman et al., 2016; Lin et al., 2016; Warner and Tissot 2012) within the whole domain, considering the maximum depth at each pixel, as suggested in (Pasquier et al. 2019, Hamman et al. 2016). The benefits of this empirical approach are that it overcomes sensitivity to the choice of the distribution and does not require a definition of the distribution parameters. By comparing the empirical distributions, we can investigate how changes in the scenario characteristics modify the frequency of the maximum inundation depths.

• In the Bibliography, items are not ordered alphabetically, nor they are given the proper stylisation.

We have fixed the bibliography for style and missing ones. We also sorted them alphabetically.

References:

A. *Shen, X., Anagnostou, E. N. (2017),A Framework to Improve Hyper-Resolution Hydrologic Simulation in Snow-Affected Regions. Journal of Hydrology, 552, 1–12. https://doi.org/10.1016/j.jhydrol.2017.05.048, 2017*

B. *Cook A., Merwade, V., (2009) Effect of topographic data, geometric configuration and modeling approach on flood inundation mapping. Journal of Hydrology, 377, 1–2, 20, 131-142 https://doi.org/10.1016/j.jhydrol.2009.08.015*

C. *K. Bradbrook, S.N. Lane, S.G. Waller, P.D. Bates, Two dimensional diffusion wave modelling of flood inundation using a simplified channel representation. Int. J. River Basin Manag. 2, 211– 223 (2004)*

D. *Bates, P. D., Dawson, R. J., Hall, J. W., Horritt, M. S., Nicholls, R. J., Wicks, J., & Hassan, M. A. A. M. (2005). Coastal Engineering, 52, 793–810.*

E. *Ahearn E.A., (2004). Scientific Investigations Report 2004-5160, https://doi.org/10.3133/sir20045160*

F. *FEMA,CT DEEP (2013). Coastal Hazards Map Viewer Information http://www.cteco.uconn.edu/viewers/coastalhazards.htm#surge*

~~Current and Future Climate~~Impact of Compound~~-~~ Flood Event ~~Flood Impact~~ on Coastal Critical Infrastructures Considering Current and Future Climate

Mariam Khanam[1], Giulia Sofia[1], Marika Koukoula[1], Rehenuma Lazin[1], Efthymios I. Nikolopoulos[2], Xinyi Shen[1], and Emmanouil N. Anagnostou[1]

[1]Civil and Environmental Engineering, University of Connecticut, Storrs, CT 06269, USA
[2]Mechanical and Civil Engineering, Florida Institute of Technology, Melbourne, FL 32901, USA

Correspondence to: Anagnostou, Emmanouil N. (emmanouil.anagnostou@uconn.edu)

Abstract. The changing climate and ~~adverse~~ anthropogenic activities raise the likelihood of damages due to compound flood hazards, triggered by the combined occurrence of extreme precipitation and storm surge during high tides, and exacerbated by sea level rise (SLR). Risk estimates associated with these extreme event scenarios are expected to be significantly higher than estimates derived from a standard evaluation of individual hazards. In this study, we present case studies of compound flood hazards affecting critical infrastructure (CI) in coastal Connecticut (USA) based on actual and synthetic (~~that is, under~~considering future climate conditions for the atmospheric forcing, sea level rise, and synthetic hurricane tracks) hurricane events, represented by heavy precipitation and surge combined with ~~high~~ tides and SLR conditions. We used the Hydrologic Engineering Center's River Analysis System (HEC-RAS), a two-dimensional hydrodynamic model to simulate the combined coastal and riverine flooding on selected CI sites. We forced a distributed hydrological model (CREST-SVAS) with weather analysis data from the Weather Research and Forecasting (WRF) model for the synthetic events and from the National Land Data Assimilation System (NLDAS) for the actual events, to derive the upstream boundary condition (flood wave) of HEC-RAS. We extracted coastal tide and surge time series for each event from the National Oceanic and Atmospheric Administration (NOAA) to use as the downstream boundary condition of HEC-RAS. The significant outcome of this study represents the evaluation of changes in flood risk for the CI sites for the various compound scenarios (under current and future climate conditions). This approach offers an estimate of the potential impact of compound hazards relative to the 100-year flood maps produced by the Federal Emergency Management Agency (FEMA), which is vital to developing mitigation strategies. In a broader sense, this study provides a framework for assessing risk factors of our modern infrastructure located in vulnerable coastal areas throughout the world.

1 Introduction

~~Almost 40 percent of people in the United States live in coastal areas with relatively dense populations (NOAA, 2013), where extreme climate events like sea level rise (SLR), storm surges, and inland rainfall play an important role in producing compound flooding and hazards (Wahl et al., 2015; Winsemius et al., 2013; Hallegatte et al., 2013; de Bruijn et al., 2017; de Bruijn et al., 2019). Changes in extreme climate events and the rise of compound flood hazards account for most of the recent increases in damage and economic impacts to society, the environment, and infrastructure (Wahl et al., 2018; Zscheischler et al., 2018), as demonstrated by the combination of unprecedented~~

inland rainfall accumulation and storm surges from hurricanes such as Harvey, Irma, Sandy, and Florence. These events were only the latest in a line of compound events, and they raise concerns about hazards previously considered independent of one another (Barnard et al., 2019; Leonard et al., 2014; Moftakhari et al., 2017; Wahl et al., 2015). When fluvial flooding combines with the co-occurrence of coastal surge and high tide, the potential for extensive inundation is much greater than from either alone, whether in the course of extreme or more frequent events (Moftakhari et al., 2017). SLR induced by climate change will further exacerbate these effects. Continuous economic growth and climate change are expected to increase these severe impacts, as well (Dottori et al., 2018; Blöschl et al., 2017).

The impacts of hurricanes such as Harvey, Irma, Sandy, Florence, and Laura are characteristic examples of hazardous storms that have affected the society and environment of coastal areas, and have damaged infrastructure, through the combination of heavy rain and storm surge. The increased frequency of such events raise concerns about compound flood hazards previously considered independent of one another (Barnard et al., 2019; Leonard et al., 2014; Moftakhari et al., 2017; Wahl et al., 2015; Zscheischler et al., 2018; Winsemius et al., 2013; Hallegatte et al., 2013; de Bruijn et al., 2017; de Bruijn et al., 2019, Bevacqua et al., 2019).

Concurrent with the rise in disaster event intensities, the elevated damage, and disruption caused by compound coastal eventsflooding (CF) to critical infrastructure (CI) and services, including electrical systems, water, and sewage treatment facilities, and the other utilities that underpin modern society, have substantial adverse socioeconomic impacts. , especially in low-lying coastal areas, where almost 40 percent of people in the United States live (NOAA, 2013).

The growing record of significant impacts from extreme events around the world (Chang et al., 2007; McEvoy et al., 2012; Ziervogel et al., 2014; FEMA, 2013; Karagiannis et al., 2017) demands adds an urgency to the immediate hardening of critical infrastructure by utilitiesneed for reassessing CI management policies based on compound impact, to help ensure flood safety and governmental agencies to improve system reliability when these major events occurrapid emergency management (Pearson et al., 2018). Globally, $2.5 trillion a year is spent on infrastructures meant to perform for decades—a lifespan that will be shortened by The uncertainty of the projected effectscurrent evolution of climate change (Dawsoncompound events translates into an even greater uncertainty concerning future damage to CI (de Bruijn et al., 20182019, Marsooli et al., 2019).

A common practice in the study of flooding is a probabilistic analysis of univariate flood drivers (such as streamflow, water level, or precipitation), independent of others. But compound events emerge from complex processes with multiple causes, and they do not conform neatly to traditional categories of extremes or current risk assessment methodologies. On the one hand, tide-surge-SLR are modelled using coastal models in isolated open environments without considering fluvial effects on the flooding. On the other, riverine models cannot capture the risk from tide-surge-SLR effects (Barnard et al., 2017). Consequently, the modelling of individual flood drivers separately mischaracterizes the true risk of flooding to coastal communities and critical infrastructure, introducing uncertainties that make the design of long-lived infrastructure much more difficult. Significant losses can result in when the designs are inadequate and ill-adapted to climate conditions.

~~The impact of climate change on tropical storms and the effects of SLR in coastal areas adds urgency to the need to revaluate management policies based on compound impact, especially on critical infrastructure, to help ensure flood safety and rapid emergency management. Marsooli et al., (2019) suggested the frequency and intensity of coastal flooding induced by hurricanes and tropical cyclones may increase significantly in the twenty-first century. In the past decades, numerous studies have been initiated to find trends in the future intensity and impact of the changes in climate. Recent research has shown spatial variability in SLR and cyclone climatology change results in differences in flood hazards across the basin and global scales (Muis et al., 2016; Marsooli et al., 2019; Vousdoukas et al., 2018).~~ Recent studies have underlined the importance of understanding and quantifying the flood ~~risks to critical infrastructure and their wider~~ impacts on ~~flood~~critical infrastructure, and their broader implications in risk management and catchment-level planning (Chang et al., 2007; McEvoy et al., 2012; Ziervogel et al., 2014; de Bruijn et al., 2019; Pearson et al., 2018; Pant et al., 2018; Dawson, 2018). ~~Few~~Some authors have ~~explored~~estimated the frequency ~~and risk assessment~~ of compound flooding and provide approaches to risk assessment based on the joint probability of precipitation and surge (Bevacqua et al., 2019; Wahl et al., 2015~~), however.~~). The spatial extent and depth of compound flooding can ~~essentially~~ vary in frequency (Quinn, et al., 2019) ~~from one location to another, and the effects of compound-event flooding (inundation and~~ if any of the component of CF is not taken into consideration while evaluating flood ~~depth) taking into account climate change impact have largely been overlooked. The uncertainty of~~ frequency. Both storm surges and heavy precipitation, and their interplay, are likely to change in the ~~current evolution of disaster damage translates into even greater uncertainty concerning~~ future ~~damage to CI. (de Bruijn~~(Field et al., ~~2019,~~2012, Dottori et al., 2018; Blöschl et al., 2017; Muis et al., 2016; Marsooli et al., 2019; Vousdoukas et al., 2018).~~2019)~~ Nonetheless, the effects of CF, considering the climate change impact, have not been thoroughly explored yet.

To deal with CF threats and challenges to coastal communities, there is a need to develop efficient frameworks for performing systematic risk analysis based on a wide range of actual and what-if scenarios of such events in current and future climate conditions. In this study, we focused on coastal power grid substations as critical infrastructure and investigated the impacts of compound flood hazard scenarios associated with tropical storms. We present a hydrologic-hydrodynamic modeling framework to evaluate the integrated impact of flood drivers causing CF by synthesising current and future scenarios. This study enables the quantitative measurement of CF hazard casted on critical infrastructures in terms of flood depth and flood extent by observing actual storm-induced floods and drawing information from synthetic scenarios. To project the combined ~~hazard, we developed a dynamic framework that investigated~~flood hazard in future climate~~-driven changes by integrating~~ conditions, we integrated the effects of SLR, tides, and synthetic ~~future climate~~ hurricane ~~events~~event simulations into the flood hazard exposure.~~ This~~

Even though past research on the assessment of damages to the power system components or other related infrastructures has proposed design and operation countermeasures and remedies (i.e. Kwasinski et al. 2009; Reed et al. 2010; Abi-Sarma and Henry, 2011; Chang et al., 2007; de Bruijn et al., 2019; Pearson et al., 2018; Pant et al., 2018; Dawson, 2018), these studies lack a comprehensive hazard assessment on power grid components, and.potential changes due to climate change.

The scenario-based analysis ~~provided a comparative flood hazard assessment that allowed us to demonstrate quantitatively the impact of compound flooding on CI in coastal areas and~~of this study formed the basis on which to address two questions:

(1) ~~How well would critical infrastructure weather a hurricane~~What are the characteristics of the tropical storm-related inundation, considering ~~a~~the compound effect of ~~concurrent~~ riverine and coastal flooding ~~during~~coinciding or not with peak high tides~~?~~

(2) Will future climate (including SLR and intensification of storms due to warmer sea surface temperatures) bring a significant increase in flood ~~risk?~~ impact for the power-grid coastal infrastructures?

The proposed framework offers a multi-dimensional strategy to quantify the potential impacts of tropical storms, thus enabling for a more resilient grid for climate change and the increasing incidence of severe weather.

We investigated these questions based on eight case studies of CI in~~ the state of~~ Connecticut (USA), distributed on the banks of coastal rivers discharging along the Long Island Sound.

2 Materials and methods

2.1 Study sites

This study focused on seven coastal river reaches (Fig. 1, Table 1), where eight power grid substations lie in proximity to riverbanks~~. The critical infrastructure at these sites is~~ and are prone to flooding caused by both ~~heavy precipitation events and~~ coastal storms (such as hurricanes~~).~~) that combine heavy precipitation and high surge. These power grid substations are coded on the map CI1 through CI8.

For each river reach adjacent to ~~the~~a CI, we developed a hydrodynamic model ~~domains~~domain, and we applied a distributed hydrological model for predicting river flows from the upstream river ~~basins~~basin. Table 1 shows the specification of each river reach, associated drainage basin, the correspondent domain extent for the hydrodynamic simulations, and the hydrological distance [distance along the flow paths] of each power grid substation from the coastline. ~~The hydrologic distance represents the distance from each CI to the coastline.~~ This distance~~ is measured along the direction of flows, and it~~ was derived using the 30m National Elevation Dataset (NED) for the continental United States (USGS 2017). ~~The considered rivers belong to watersheds ranging from 10 to 300 km2 in extent. For this study, the simulated domains ranged from 3.7 to 8.3 km in river length and 2.2 and 20.7 km2 in area. The substations were coded from CI1 to CI8. Except for CI4 and CI5, which are within the same simulation domain, each substation has an independent domain.~~

Among the case study sites, two CIs are relatively inland [CI3 and CI4] (table 1: see hydrologic distance. Figure 1: see coastal boundary), nonetheless all the sites are included within the Coastal Area as defined by Connecticut General Statute (CGS) 22a-94(a) [https://www.cga.ct.gov/current/pub/chap_444.htm#sec_22a-94]. The considered rivers belong to watersheds ranging from 10 to 300 km^2 basin area, which are sub-basins of the Connecticut River basin. The hydrodynamic model simulation domains ranged from 3.7 to 8.3 km in river length and 2.2 and 20.7 km^2 in area.

2.2 Simulation framework

To evaluate the effect of compound events, we selected four tropical storms: two actual hurricanes (Sandy and Irene) that hit Connecticut (Sandy and Irene) , and two synthetic hurricanesscenarios based on actual hurricanes Sandy and Florence. We subjected the latter two events to different atmospheric conditions leading to landfall scenarios with greater impacts, with the Sandy scenario representing hurricane Sandy under future climate atmospheric and sea surface conditions (Lackmann 2015). Both Irene (August 21–28, 2011) and Sandy (October 22–November 2, 2012) reached category 3, but they made landfall in Connecticut as category 1 hurricanes. To investigate the impact of floods under The synthetic simulations (Chapt. 2.2.1) include different climate and compound effectatmospheric conditions leading to landfall scenarios associated with river flows, tides, stormgreater impacts. The Sandy synthetic scenario represents hurricane Sandy under future climate and sea surface conditions (Lackmann 2015), while the synthetic scenarios for Florence were based on simulated surge, tide condition and future SLR (see Chapt. 2.2.1 and 2.3).

To investigate the impact of floods of the various scenarios, we devised a combined hydrological (subsection b, below) and hydrodynamical (subsection cChapt. 2.2.2) and hydrodynamic (Chapt. 2.2.3) modeling framework (Figure 2), forced with weather reanalysis data and geospatial data for the actual events, and a numerical weather prediction model (subsection a) for the synthetic events (that is, synthetic hurricane Florence and future hurricane Sandy).

2.2.1 Atmospheric simulations

To simulate the two synthetic Sandy and Florence hurricane events, we used the Weather Research and Forecasting (WRF) system (Powers et al., 2017; SkamarockShamarock et al., 2007). For the synthetic hurricane Florence event, we used a hurricane track forecast by the National Oceanic and Atmospheric Administration (NOAA)), that showed landfall in Long Island and Connecticut, and we based synthetic Sandy on future climate conditions (post 2100). For the soil type and texture input in the WRF model for both synthetic storm simulations, we used USGS GMTED2010 30-arc-second (Danielson and Gesch 2011) DEM for the topography, Noah-modified 21-category IGBP-MODIS (Friedl et al., 2010) for land use and vegetation input, and Hybrid STATSGO/FAO (30-second) (FAO 1991) for soil characteristics.

More specifically, as of September 6, 2018, according to the Global Forecast System (GFS) forecasts of the National CentersCenter for Environmental Prediction (NCEP) (Higgins 2000), the prediction for one of the tracks of Florence), showed landfall in Long Island and Connecticut on September 14 as a category 1 hurricane. (Higgins 2000).

We based synthetic hurricane Sandy event on future climate conditions (post-2100).

For the soil type and texture input in the WRF model for both synthetic storm simulations, we used the USGS GMTED2010 30-arc-second (Danielson and Gesch 2011) Digital Elevation Model for the topography, the Noah-modified 21-category IGBP-MODIS (Friedl et al., 2010) for land use, and vegetation input, and the Hybrid STATSGO/FAO (30-second) (FAO 1991) for soil characteristics.

To simulate the synthetic hurricane Florence with WRF, we used thesethe GFS forecasts at 0.25° x 0.25° spatial resolution as initial and boundary conditions. We used a three-grid setup with a coarse external domain of 18 km spatial resolution and two nested domains with 6 km and 2 km horizontal grid spacing, respectively. Two-way nesting was activated for both inner domains. Vertically, the domains stretched up to 50 mb with 28 layers. We parameterized convective activity on the outer (resolution of 18 km) and the first nested (resolution of 6 km) domain using the Grell 3D ensemble scheme (Grell and Devenyi 2002). Further details on the model setup are presented in Table 2.

For the future hurricane Sandy scenario, we used the hurricane Sandy simulations under future climate conditions (after 2100) by Lackman (2015), who used a three-grid setup at spatial resolutions of 54, 18, and 6 km. We defined initial and boundary conditions by altering the European Centre for Medium-Range Weather Forecasts (ECMWF) interim reanalysis (Dee et al., 2011) data, based on five General Circulation Model (GCM)-projected, late-century thermodynamic changes derived from the IPCC (Intergovernmental Panel on Climate Change) AR4 A2 emissions scenario (Meehl et al., 2017). A complete description of the modeling framework is provided by Lackman (2015).

2.2.2 Hydrological ~~modelling~~modeling

To account for the river inflow (upstream boundary condition), we ~~devised~~ applied a physically-based distributed hydrological model [CREST-SVAS (Coupled Routing and Excess Storage–Soil–Vegetation–Atmosphere–Snow~~)~~ ~~(~~)] described in Shen and Anagnostou (2017~~), a physically-based distributed hydrological model.~~).

To simulate river discharges for the synthetic hurricanes (Florence and future Sandy), we used the WRF simulations at 6-km/hourly spatiotemporal resolution, as described above. To force the hydrological model for the actual events (Sandy and Irene), we used data from Phase 2 of the North American Land Data Assimilation System (NLDAS-2) (Xia et al., 2012) dataset. NLDAS-2 is a gridded dataset derived from bias-corrected reanalysis and in situ observation data, with a one-eighth-degree grid resolution and an hourly temporal resolution, available from January 1, 1979, to the present day. We derived the precipitation from daily rain gauge data over the continental United States, and all other forcing data came from the North American Regional Reanalysis (NARR) by NCEP (Higgins 2000), to which we applied bias and vertical corrections. ~~In CREST-SVAS, we resampled the direct runoff of each grid at 500 m resolution to 30 m routing in coastal basins of the small drainage area (see Table 1) to improve the accuracy of river flow estimation.~~ To reduce the computational effort, we performed the hydrological simulation using a hydrologically conditioned 30 m spatial resolution ~~digital elevation model (DEM)~~DEM (USGS 2017).

~~Also included in~~The hydrologic simulation include the ~~hydrological model was~~use of land use and land cover ~~(LULC)~~ information retrieved from the Moderate Resolution Imaging Spectroradiometer (“MOD12Q1” from MODIS~~).~~) (Friedl et al., 2015~~)~~). To compensate for the coarse resolution (500 m) of these data, we obtained imperviousness ratios using Connecticut’s Changing Landscape (CCL) database and the National Land Cover Database (NLCD) at 30 m resolution. In CREST-SVAS, the land surface process was simulated by solving the coupled water and energy balances to generate streamflow at hourly time steps at the outlet of the studied watershed. ~~The model has been validated (Shen and Anagnostou, 2017; Hardesty et al., 2018) in river basins within Connecticut, where all the watersheds simulated in this study reside~~CREST-SVAS was calibrated and validated for the whole Connecticut river basin [that contains all the investigated sites] with an NSCE of 0.63 (Shen and Anagnostou, 2017). We further validated the model considering hourly flows in two locations within the Housatonic River and Naugatuck River watersheds with an NSCE of 0.69 (Hardesty et al., 2018). The quality measures indicate a satisfactory model performance at the watershed scale over the topographic region that collectively include our study sites.

2.2.3 Hydrodynamic modellingmodeling

To assess the flood hazard in terms of extent and the maximum depth of the flood, we implemented the Hydrologic Engineering Center's River Analysis System (HEC-RAS), developing individual two-dimensional model domains for eacharound the CI location. We generatedExcept for CI4 and CI5, which are within the same simulation grids from 1 m LiDARdomain, each substation has an independent domain.

The inundation maps are derived using a 1m LIDAR DEM archived in Connecticut Environmental Conditions Online (CtECO 2016), including building footprints to) taken as base maps for the study reaches. To better represent better the impacts of urban establishments on inundation dynamics. , solid urban features such as houses and buildings, which obstruct the flow of stormwater, were added to the bare-earth DEM. For this, we considered the building footprints from (CtECO, 2012) and identified positions of buildings and houses in the DEM by increasing the elevation of the pixels within the building footprint polygons by an arbitrary height of 4.5 m, assuming one-story buildings.

The considered locations have no bathymetric (underwater topography) data represented in the DEM. In general, the impact of inclusion/exclusion of bathymetry data on the hydrodynamic model simulations will vary according to the river size and event severity (Cook & Merwade 2009). For the investigated events in this study flood risk is mainly dominated by defence overflow and defence breaching. This means that we do not require detailed bathymetric information in the upstream main channel, thereby considerably simplifying the modeling problem (Bates et al. 2013). Therefore, we did not represent the flow of water in the main channel. Rather boundary conditions were given as time series of water surface elevation imposed along the defence crests.

To reduce the computation time, we created a 2D mesh grid at 10 m background resolution, enforced with breaklines to intensify the riverbank and other areas with a large elevation gradient up to 1 m resolution. HEC-RAS allowed a gradual mesh distribution around the breaklines, preserving most of the information from the 1 m DEM. For the hydrodynamic model, we retrieved 2011 land cover classification data from the National Land Cover Database (NLCD). The upstream boundary condition was provided by CREST-SVAS, and the downstream boundary condition (coastal water level, including coastal tide, storm surge, and sea level) was derived from National Water Level Observation Network (NWLON) data, provided by NOAA. These data are available as actual observations and predictions at intervals of six minutes to one hour. Figure 3 provides an example of one of the sites, showing the upstream and downstream boundaries, along with a map overlay of flooded areas of five (SD1–SD5) scenarios (see below) for CI2. We initiated the simulation with a warmup period of 12 hours to achieve stability. We chose the full momentum scheme in HEC-RAS and extracted hourly output from the simulation.

The model parameters were calibrated to obtain realistic water depths and extents, as compared to reference data collected for Sandy. To validate the hydrodynamic model simulations, we used surveyed HWMs (high water marks) (Koenig et al., 2016) collected by the United States Geological Survey (USGS) after hurricane Sandy at 15 selected locations spread across the simulation domains. HWMs are frequently used to calibrate and validate model outputs and satellite-based observations of flood depth (Bunya et al. ,2010; Cañizares and Irish 2008; Cariolet, 2010; Chang et al., 2007; Hostache et al. 2009; McEvoy et al., 2012; Pearson et al., 2018; Schumann et al., 2008; Schumann et al., 2007; Schumann et al., 2007; Ziervogel et al., 2014). As for the flood extent, we further validated the model against the most accurate available information on the 2D extent and maximum depth of storm surge for Sandy (FEMA, CT DEEP, 2013), created from field-verified HWMs and Storm Surge Sensor data from the USGS.

An HWM does not necessarily indicate the maximum flood depth; rather, it can be a mark from a lower depth that lasts long enough to leave a trail. Based on this understanding, we compared the HWMs against the simulated flood depths~~.~~ within a 10x10m radius around the high water marks, also to avoid issues due to the presence of buildings in the DEM (Boxplots in Fig. 4). The simulated depths demonstrated reasonable agreement with the collected HWM values (Figure 4), with the model ~~tending to show a slight overestimation in all cases. In the current study, this limitation came mostly from the uncertainty in the LiDAR DEMs. LiDAR data, especially in large and deep channels, do not provide a suitable representation of the submerged channel bed, and this results in an underestimation of channel conveyance capacity and subsequent overestimation of the flood extent. In this case,~~showing a slight overestimation. In this case, the systematic error fell within values of expected precision, implying a consistent positive bias in the simulations not strong enough to hinder the results.

Figure 5 shows a visual comparison for CI1 and CI2 between the simulated inundation (Fig.5 a, c), and the reference extent (Fig. 5 d,e). A slight overestimation of the flood level, ranging between 0.2 and 0.4 m, with a precision of 0.2 m or less, is observed for the inundation depths at the displayed locations, which is consistent with the results obtained locally, at the HWM locations (Fig. 4). Taking into consideration the accuracy of the inundation depth, the declared DEM accuracy (vertical RMSE ~0.3m), and the simplified modeling problem concerning bathymetry, the accuracy of the flood extent assessment was judged satisfactory.

2.3 Compound scenarios

We ~~modelled~~modeled four types of synthetic compound event scenarios ~~besides the simulation of the~~, as well as actual events by (1) simulating the synthetic hurricanes; (2) introducing a climate change factor, in the form of SLR (~0.6 m), as projected for 2050, as a prediction for intermediate low probability (CIRCA 2017); (3) shifting the surge timing to make the surge peak-level occurring at local high tide ~~coincides with the storm surge~~; and (4) combining the SLR with the high tide condition. The combination of these four ~~scenario~~event types yielded nine ~~compound scenarios. The following describes the simulated scenarios~~simulations, hereby coded as IR or SD for ~~the three~~hurricanes Irene and Sandy, and FL for the synthetic hurricane ~~events.~~Florence.

~~IR1 and IR2 were the two~~Two scenarios were created for hurricane Irene. IR1 was the actual hurricane Irene, that made landfall in Connecticut during high tide, and IR2 was the IR1 scenario with future SLR added to the tidal water level ~~at the~~as a downstream boundary ~~of~~condition in HEC-RAS. ~~A point to note is that hurricane Irene made landfall in Connecticut during high tides.~~

For hurricane Sandy, we generated five scenarios. SD1 was the actual Sandy. For SD2, we shifted the peak high tide ~~time series~~ to coincide with the ~~peak~~ maximum storm surge~~. SD3 was~~ recorded, as derived from the local NOAA stations (hereafter referred to 'shifted tide water levels'). We further added SLR to the shifted tide water levels from SD2 to create the third scenario ~~SD2 with SLR added to the modified total water level from NOAA.~~(SD3). The remaining two scenarios for hurricane Sandy represented future climate conditions. Specifically, SD4 was the future hurricane scenario simulated with the GFS (Chapt. 2.2.1) and shifted ~~NOAA~~ tidal water ~~levels~~level. SD5 was the future Sandy with shifted tide water levels and SLR.

For the synthetic hurricane Florence event, we simulated two scenarios. FL1 was the synthetic Florence event, based on the GFS track that gave landfall in Connecticut and Long Island~~.~~ (Chapt. 2.2.1). FL2 was ~~scenario FL1~~the same synthetic event, with SLR added to the coastal water levels.

Table 3 shows, for each scenario, the basin-averaged event accumulated precipitation (mm) and the simulated peak flow (m3/s) ~~at the basin outlets~~used as an upstream boundary condition in HEC-RAS, along with the recurrence interval of the peak flows derived using a Log-Pearson probability distribution fitted using yearly maxima from the long-term simulated flows (1979-2019) from CREST. ~~We have used the Log- Pearson probability distribution method to fit the annual maximum flows. The flood frequency curves are then used to determine the corresponding recurrence interval of the peak flows for different scenarios.~~ This shows how significant the precipitation forcing was for each considered scenario. For CI1, for example, the future Sandy (~~SD 4~~SD4/5) scenario, with a peak flow of 242.4 m3/s, was the most extreme event with a recurrence interval of 316 ~~year~~years, followed by Irene (158.5 m3/s) and Florence (51.3m3/s) with a recurrence interval of 56 and 2 ~~year consecutively~~years respectively, whereas, for CI8, Florence and future Sandy had similar magnitudes with peak flows of 93.1m3/s (6) and 94.7m3/s (6), respectively. In table ~~4~~3, we have summarised the maximum total water level (tide & surge) used in the model at the downstream of the study sites for all the scenarios. This table represents the change in the severity of the coastal component of the compound scenarios concerning added challenges like shifted tide and SLR. For example, for CI3, the total water level increases 1m with the shifted tide (SD2/ SD4~~)~~)), and with SLR it becomes 4.4 m.

2.4 Compound flood hazard analysis

We investigated the compound effect of the different events by ~~quantifying~~comparing flood area ~~extent~~extents and flood ~~level differences in the coastal flood hazard estimates.~~depths for each event. For the flood area extent, we used as a baseline the 100-year flood maps~~.~~ provided by FEMA. The distance correlation index (dCorr) (Székely et al; 2007) has been used to identify the correlation of the differences between simulated and FEMA extent and compound events' parameters [flow and total water level peak]. dCorr values range from 0 to 1 expressing the dependence between two independent variables. The closer the value to 1 is the stronger the dependency would be, and zero implies that the two variables in question are statistically independent. dCorr can depict the non-monotonic associations of the variables and declare the dCorr value is zero if only the variables are statistically independent.

For the flood level differences, we considered the overall distribution of water depths across the domain of the CI sites and investigated the time series of water depth at each location (Figure ~~5~~6 is an example of the simulated flood depth during the scenarios of Sandy (SD1- SD5) over time for CI2).

~~Using~~To evaluate the ~~time series~~flood hazard in terms of flood ~~levels~~ depth, we computed a Cumulative Distribution Function (CDF) to shows the probability that the flood depth will attain a value less than or equal to each measured value. We estimated the CDF using all the depth values of all the grid of simulation domain, for the time step when the inundation was maximum. We evaluated the depth empirical exceedance probability (Hanman et al., 2016; Lin et al., 2016; Warner and ~~specified threshold~~Tissot 2012) within the whole domain, considering the maximum depth at each pixel, as suggested in (Pasquier et al. 2019, Hamman et al. 2016). The benefits of this empirical approach are that it overcomes sensitivity to the choice of the distribution and does not require a definition of the distribution parameters. By comparing the empirical distributions, we can investigate how changes in the scenario characteristics modify the frequency of the maximum inundation depths~~, we determined the time periods when flooding exceeded these threshold levels.~~.

The study further looked at whether the depth of water at a station would change for various scenarios. Figure 6 shows an example of the flood depth over simulated time at CI3 for the scenarios of Sandy. Pre-defined critical water levels were investigated for each station, as hypothetical values representing the height between the floor and the critical electric system in the station. Specifically, we considered 0.5 m, 1.5 m, and 2.5 m for threshold levels~~, which represented possible CI levels. For each threshold level~~. As a measure of the potential threat to the electric infrastructure, we determined the percentage of time that the flood ~~in a 24-hour window that inundation~~level was over ~~the~~ each specific threshold (Figure ~~5; red rectangle). We~~7). This data was then used to assess potential flooding problems associated with on-site inundation: we associated the changes in risk posed to the CI from the different examined scenarios ~~with~~based on the changes in those percentages. ~~This analysis indicated as to whether and for how long CI components could be below floodwater.~~

3 Results and ~~Discussions~~Discussion

3.1 Flood extent

~~We compared~~ The inundation extents shown in figure 6 represent an aggregation of the ~~simulated~~overall runs rather than a specific simulation time, and it represents the extent reached when all pixels had the maximum inundation depth. Total flood ~~extents to the FEMA 100-year flood zone for all the scenarios (Table 4, Figure 6a–c). Inundated areas~~ extent ranged between less than 1 km^2 to more than 7 km^2, with a minimum extent of 0.4 km^2 for the actual Sandy (SD1) at C8, ~~to more than 7 km2, with a~~ and a maximum extent of 7.1 km^2 for the future Sandy (SD5) at C3. The results showed consistent agreement that the flood extent increased with increasing intensity of the event and an increase in the recurrence intervals of the flows (Table 3).

Changes across the study sites relative to the FEMA ~~extent~~100-year flood extend (Table 4, Figure 7a–c) ranged from –87.8% (for CI8 for SD1) to 192.2% (for CI2 for IR2). ~~The results showed strong agreement that the flood extents increased with increasing intensity of the events and increase in their recurrence intervals (explained in Table 3). The~~ Overall, the sites with a return period of fewer than 100 years, ~~as expected,~~ showed consistently less flooding than ~~shown on~~that of the FEMA map, a finding best represented by the comparison of actual events ~~(~~, such as IR1.

Since the model performance shows a good agreement with the actual flood extents, and ~~IR2);~~the HWMs (Chapt.2.2.3), our results suggest that FEMA's flood maps do not fully capture the flood extent at least for ~~example, as shown~~some locations. Similar findings were reported in ~~Table 4, the CI1–CI8 for IR1~~Jordi et al. (2019), Wang et al. (2014) and ~~SD1 had less inundated areas than shown~~Xian et al. (2005), where tens of meter-scale absolute differences were found between the FEMA estimated flood extent for hurricane Sandy. The strength of correlation (dCorr) between changes in the upstream (flow peak) or downstream (surge peak) components, and the absolute differences with FEMA extent, gives an idea of the importance of each single driver of change. For the cases investigated in this study, the percentage difference mostly depends on the FEMA 100-year flood map, which resonates positively with the return period of surge: surge height explains more than 80% of the variation in the differences to FEMA extent (dcorr=0.8 in median). CI6 appears to be the sites where the surge has the strongest correlation with the absolute difference in flood extent, as compared to FEMA maps. The differences with FEMA maps are less related to the peak flows in Table 3. (median correlation 0.5, with max correlation recorded for CI3). As expected, the correlation with surge increases at the decreasing of the hydrologic distance to the coast, while the correlation with the flow increases the further a site is from the coast, even though this relationship is not linear.

As we proceeded with the synthetic scenarios, adding compound and future challengesclimate, the results indicated the supplementaryadditional impacts of the joint flood drivers (shifted tide, surge, SLR). Therefore, the percentage change was the most useful basis for comparison of the different scenarios of an event.

The shift in For the same event, peak storm-tide time (levels occurring near local high tide (i.e. SD2) resulted in more flooding than resulted fromthat of events happening at low-tide (like actual Sandy (, SD1). The increase in floodClimate change related SLR exacerbates extreme event inundation relative to a fixed extent (FEMA) with variability that ranged from 8.3% (CI4/5) to as high as 425% (CI8), showing how severe Sandy would have been if it had hit). CI8 is the coastline during high tide. The hydrologicalsite hydrologically closer to the coast (see hydrologic distance (in Table 1) of CI8 was only 2.9 km from the coastline,), making it the closest to the shore and the most susceptible to the altered scenario. ShiftedNonetheless, the shifted tide increased the inundation relative to the FEMA 100-year flood map also for CI2 and CI4/5, suggesting shifted tide time alone can alter the traditionally derived 100-year flood zone significantly..

The effects of compound events emerged drastically with the combination of both shifted tide and SLR. Except forWith the exception of CI3 and CI8, all theother CIs showed an increase in the percentage change from FEMA (Table 4). In comparison to SD1, SD3 showedexhibited increased inundation for all the CIs. The inundated area was about 146% more (1.9 km^2) for SD3 than SD1 (0.9 km^2) for CI1, for example. The flowsriver flood peak for hurricane Sandy had a recurrence interval of about two years, but the flood hazard associated with themthis event became more devastating with the if simulated in a compound effect. way, including SLR and shifted tide. This result suggests that events of lower river flood severity (from less rain accumulations) can produce aggravating impact, as the intensity of major storm surges increases due to shifted timing and SLR.

For the synthetic hurricane Florence and hurricane Irene, we saw an increased flooded area in comparison to FEMA (Table 4); for CI2, for example, the increase was almost 200% from IR1 to IR2. These results make it very clearAgain, this result confirms that accounting for river peak flow frequency cannot be the only measure to translatealone does not effectively capture the severity of a flood hazard. in the case of coastal locations.

For all the study sites for future Sandy, we saw consistent increases in flood extent (Table 4) from SD2 to SD4 and SD3 to SD5. Between SD2/SD3 and SD4/SD5, the only difference was the future projection of the flow. In comparison to the FEMA map, the percentage change ranged from –22.3 to +123.7. CI1, CI7, and CI8 for SD4 have less inundation than the FEMA 100-year map. This may be an indication of the significance of individual flood components specific to one site. For those sites, river flow might not be the most significant component of the flood. When we look at the hydrologic distances in table 1 CI1 and CI8 are closer to the coastline, making them more prone to coastal flooding than fluvial flooding. When we looked at SD5 (which added SLR), all the sites except CI8 showed more flooding than the FEMA 100-year flood map. Although CI8 had an increase of 22% in inundation compared to SD4.

When we compare the worst-case future events (SD5 and IR2) to actual events (SD1 and IR1), we can see ~~extreme~~major changes in flood extents. The flood extent in all locations increased by about 60% on average for future Sandy with both SLR and coinciding tide (SD5) in comparison to the actual Sandy (SD1), with the highest impact in CI8 (+148%). Looking at Irene, the worst-case future scenario (IR2) increased the flood extent by about 30% on average for all locations compared to the actual event (IR2), with the highest impact in CI2 (101%). Among all the events, Florence had the lowest expected changes, between the current climate scenario (FL1) and the future one (FL2). One must note that hurricane Florence had no actual impact in the study area; the simulation for this event was based on a ~~possible~~hurricane track forecast by GFS, ~~showing it could~~which if materialized would have produced a flood inundation of almost 5 km^2 in CI3, and ~~that~~ this extent could have increased by about 20% in the worst-case future scenario (FL2) that ~~included~~includes shifted tide and SLR. Five of the CIs were ~~exposed~~ outside the FEMA 100-year flood zone, but they present flooding for FL1 and SD3. For FL2 all of the study sites were ~~exposed to~~ more ~~vulnerability~~vulnerable (positive % change~~)~~), as compared to the FEMA map ~~and~~. Similar findings are presented for SD5, ~~all~~with the ~~sites except~~exception of CI8.

3.2 Flood depths over the domain

~~To evaluate~~ While flooding occurs in all the ~~flood hazard in terms of flood~~ presented scenarios, both extent and depth~~,~~ ~~we analysed~~ vary greatly between the ~~cumulative distribution function (CDF) of maximum flood depths within the simulation domain. CDFs are effective for comparing flood damage among~~ different ~~events (Hanman et al., 2016; Lin et al., 2016; Warner and Tissot 2012). From our analysis of the CDFs (Figure 7) emerged the finding that the dependence among the combined effect of coastal water level, fluvial flow, and tide strongly influenced the joint~~ simulations. Depth is important to consider while preparing for risk management as it is used in determining flood damage.

The CDFs of water depth ~~probability~~for the whole domain (Figure 8), confirm that the water depths derived for coupled events (i.e. high tide coinciding with surge peak, or SLR and future climate) are generally higher than those derived from events with independent drivers Note that for some cases (i.e. IR1 and~~, in turn,~~ IR2, for CI2 in Fig. 8) water depths increase very consistently as SLR increase. Larges changes in the CDFs appears for lower water depths. Thus, regions with generally lower hazard (depth), will likely experiences larger impacts under SLR. Results also confirm that scenarios with simultaneous high values for all these parameters implicated a higher vulnerability of the CIs. ~~For the same probability, the flood depth was greater for~~ Comparing these changes in pairs [i.e. IR1 vs IR2, or SD1 vs SD3] also highlights that compound scenarios~~. This behaviour was consistent~~ changes in the frequency of extreme values that go far beyond the average are much more pronounced than the related changes of the median depths (cumulative probability=0.50). In particular, it may be asserted that more expressed changes in extremes could lead to corresponding "hazard shift" for all CIs, as represented in Figure ~~7.~~8.

These results suggest that fluvial flow is not the only driver determining flood risk. Actual Irene (IR1) and synthetic Florence (FL) had higher river flood return periods than did actual Sandy (SD1) (Table 2). Nonetheless, the CDFs of the flood depth showed different behavior in terms of severity. For CI1, for example, IR1 had higher probabilities for lower depth, followed by SD1 and FL1. In CI8, SD1 had higher probabilities for lower values of depth. These findings highlight that neither the severity of rainfall, nor the magnitude of river ~~flows to control~~flow controls the flood~~ extent and flooded area~~ characteristics, which are, rather, controlled by additional factors, such as storm surge, high tides, topography, and location of the site. CI7, for example, which is more coastal than the other CIs, presented increasing flood depth due to tidal timing.

As expected, and as previously highlighted when considering the flood extent (Table 4), climate played an important role in flood hazard changes. Furthermore, the effect of SLR was also evident for all the events (IR, SD, and FL), increasing the flood depth for the same exceedance probability. For CI6, for example, the 50% exceedance corresponded to ~1 m depth of floodwater for IR1, increasing to ~1.5 m for IR2. For the CI4 and CI5 sites, for exceedance of 20%, actual Irene produced ~2 m of flood depth, whereas with SLR it was ~2.5 m. Another way to put it is that, for CI4/5, IR1 had an exceedance of ~20% for a flood depth of 2 m, whereas IR2 had an increased exceedance level of 40%. Similarly, for 50% exceedance, FL1 and FL2 corresponded to 1.5 m and 2 m depth of floodwater, respectively, and we ~~also~~ saw the trend for the Sandy event scenarios (SD2–SD3; SD4–SD5~~). In short, this trend could be seen for almost all the sites and is an indication of how a projected increase of SLR due to climate change might affect the risk of flood hazard at a location~~) as well.

This analysis highlighted that the timing of a storm is also crucial. The changes from SD1 to SD2 showed very well the impact of the shifted tide for all the sites. For CI3, for example, the 1 m flood depth had an exceedance of ~88% for SD2, whereas it was only ~23% for SD1.

~~These findings show~~Analysis of the overall flood depth across the whole domain shows that the coincidence of fluvial flood, high tide, and storm surge results in a significant increase in flood risk. SD3 and SD5 had all the components of a compound flood and comparing them with SD1 gave us a clear idea of how severe a compound event can be in the future. CI3, for example, had exceedance levels of almost 30%, 85%, and 90%, respectively, for SD1, SD3, and SD5 for a flood depth of 1 m. This suggests the compound effect increases the intensity of the flood hazard.

3.3 Local risk for CI

Much of the flood damage in CI is incurred by components being submerged for a long period. Investigating the duration of the flood depth at the CI location (Figure ~~8~~9) should be considered in planning for any protective measures, such as elevating or waterproofing equipment. If a critical infrastructure shows ~~for each CI the percentage of the time~~0%, it means that ~~selected~~ for that scenario/event the water ~~level thresholds were exceeded. CI1 was never flooded for any~~ didn't reach the substation at all, at least during the simulated timeframe. This could be due to the water flooding other upstream locations, and therefore draining away from the station, or because the topography of the landscape actually prevented water from reaching the area for some specific events.

According to our analysis, none of the scenarios~~.~~ has an actual impact on CI1. For the other CIs, ~~in comparisons of~~comparing individual events we could see an increase in risk due to the ~~added~~ compound hazard scenarios—that is, shifted tide and SLR. Important to note is that, for most of the sites, the compound risk due to SLR and tide timing was always higher for the lower water-level thresholds (0.5 m). This implies a higher risk for CI components currently positioned closer to the ground. ~~Much of the flood damage in CI is incurred by components being underwater for a longer time. The results of the analysis (Figure 8) should be considered in planning for any protective measures, such as elevating or waterproofing equipment.~~ Damage to the CI components is dictated by both the flood depth and the duration of submergence. The suggested high values of risk [increase percentage in ~~time-specific depths are maintained~~inundation duration] (Figure ~~8) also~~9) further imply differences in the timing of repairs. ~~Therefore, damage to the CI components is dictated by both the flood depth and the duration of submergence.~~ In the cases of CI7 and CI8 (Figure ~~8~~9), the CIs remained submerged ~~in~~with 0.5 m of water for about 20% of the event period for actual Sandy, but for the worst-case future Sandy scenario, ~~we found~~ the ~~time of submergence increased to~~location was flooded for more than 90% of the event ~~period~~duration. This demonstrates the increased flood risk to which future climate conditions expose CI.

Another important insight was provided by the hurricane Florence scenarios. As mentioned earlier, Florence did not affect the study area, although an early GFS storm forecast track predicted landfall in Long Island and Connecticut. For this event, the estimated measure of risk was about 20%, and it was shown to increase to up to 40% for the lower water depth (0.5 m) threshold in some locations. The result of the simulated scenario allows for an assessment of potential damage and for an identification of equipment that might be affected by future events under current climatic conditions. In this regard, comparing the results for the different CIs during the Sandy scenarios revealed an interesting pattern. While we might have expected a greater impact over the whole domain when shifting the tide (Figure ~~8~~9, Table. 3), we found ~~instead~~ different impacts in the ~~different~~ CI locations. Notably, the risk appeared lower when the tides were shifted (Fig. ~~8~~9) for some of the CIs (for example, CI5 and CI7). This can be explained by the fact that higher water levels in the domain were changing the water flows, allowing the flood to follow different drainable ways. This can be a very useful piece of information for deciding whether to and where to take measures in terms of flood occurrence and potentially relocating CIs to avoid catastrophic compound flood events.

From table 1 we can see that CI8 is the closest to the coastline followed by CI7, CI6, and CI5. From figure 9 we can see that all the CIs that are closer to the coastline are susceptible to changes in the downstream water level condition (Shifted tide/ SLR) (Table 3). CI4 is the farthest from the coast followed by CI3. Both the CIs show minimal response to changes in the coastal water level compared to CI5/ CI6/ CI7. This analysis gives us conclusive evidence of risk associated with the location of the CI from the coastline.

4 Concluding Remarks

Preparing for the challenges posed by climate change requires understanding of current actual, possible and future scenario of tropical storm impacts, and a correct understanding of the hazard imposed by compound flooding. In this work we have developed and implemented a modeling framework that allows to address this task, focusing on coastal electric grid infrastructure (substations). To date, the design of these facilities typically has assumed the current climatic conditions. However, a changing climate, as well as co-occurrence of compound drivers, and the resulting more extreme weather events mean those climate bands are becoming outdated, leaving infrastructure operating outside of its tolerance levels.

We explored a range of actual and synthetic hurricane scenarios, offering a system that could inform short- and long-term decisions. For the short-term decision, the framework allowed to investigate the characteristics of the hurricane-related inundation, considering the compound effect of riverine and coastal flooding coinciding, or not, with peak high tides. Generally, hurricanes affect large areas, and the specific locations at which damage will occur are often difficult to anticipate. Simulation of different scenarios can provide system operators with the ability to prepare for damage and respond quickly once it has occurred—for example, by pre-positioning repair crews. Furthermore, by simulating the impact using possible storm paths, the framework allows us to understand the potential impacts on the CI. The framework proposed in this study evaluates the extent of flood nearby a critical coastal infrastructure caused by possible extreme compound events. Each type of infrastructure system has specific elements vulnerable to specific water levels; we map those hazard infrastructure intersections where risks will be exacerbated by climate change or compound eventsFrom table 1 we can see that CI8 is the closest to the coastline followed by CI7, CI6, and CI5. From figure 8 we can see that all the CIs that are closer to the coastline are susceptible to changes in the downstream water level condition (Shifted tide/ SLR) (Table 4). CI4 is the farthest from the coast followed by CI3. Both the CIs show minimal response to changes in the coastal water level compared to CI5/ CI6/ CI7. This analysis gives us conclusive evidence of risk associated with the location of the CI from the coastline.

4 Concluding Remarks

This study evaluated the compound effect of different flood drivers (rainfall, surge, SLR, tides) for critical infrastructure in coastal areas, based on case studies of actual and synthetic hurricane events in the north-eastern United States. The proposed framework offers an approach to estimate the potential impacts of extreme compound hazards, which is vital for developing mitigation strategies. The framework will allow researchers and stakeholders to analyse the effects of combined hazards and prepare to take necessary measures to protect the vulnerable infrastructure within the flood zone.

The findings of this study can support flood mitigation; the FEMA 100-year map is used for designing infrastructure and for making decisions on flood mitigation and flood insurance. Our Nonetheless, these maps must be updated because flood risk is not static; changes in hydrology, topography, and land development all have an impact on flood conditions. The results, however, show this map does not account for the impacts posed by simultaneous conditions, such as high tide and river flows, or for future climate impacts. They show howthat the vulnerability of each substation is linked to the different stormsstorms' characteristics, and how this variesthey vary depending on the distance from the coast—that is, inland substations are less affected by surge and SLR and more affected by rainfall accumulation events (such as Irene). The findings of this study highlight that rising seas will allow storm surges to inundate areas farther inland and that flood hazard is likely to grow as seas rise and storm surges become deeper. The results also highlight that tide-surge-SLR effects modeled using only coastal models in isolated open environments without considering fluvial effects on the flooding, or riverine models without appropriate downstream boundary conditions cannot capture the risk from tide-surge-SLR effects. The variability in flood extent among scenarios implies that the modeling of individual flood drivers separately can mischaracterize the true risk of flooding to coastal communities and critical infrastructure, introducing uncertainties that make the design of long-lived infrastructure much more difficult. Significant losses can result in when the designs are inadequate and ill-adapted to climate conditions.

This study also shows that, for some locations, FEMA maps significantly underestimate the actual storm surge risk to structures near the shore relative to structures further inland, and it generally does not account for the impacts posed by simultaneous conditions, such as high tide and river flows, or for future climate impacts.

The inundation maps, as well as the depth distributions, highlight how climate change is expected to lead to increased flooding in many sites, due to rising sea levels and changing precipitation patterns. The impacts will be felt most acutely along the coasts, but our results show a significant increase also for the more inland locations, as heavy and more frequent rain events increase the risk of flash floods and riverine flooding events. The provided framework can produce inundation maps that would allow improving the CIs' resiliency in the face of natural disasters, independently from the mapping done for insurance purposes. Critical infrastructures are usually positioned by following the FEMA 100-year flood zone map. Areas outside the designated zones generally either do not have flood mitigation plans, and stand without any protection, or plans based on critical flood depths derived from FEMA zone areas. In this study, however, we see an increase in the exposed (flooded) areas for future climate scenarios, as well as some under- and overestimation as compared to FEMA maps. We also show how the flood depth exceedance probability at a location can essentially increase during compound flooding and shift due to climate changes. This further suggests the need to develop, update improved criteria for recognizing the effects of existing and planned protection measurements, such as relocating equipment or Cis, where warranted.

Future research should consider improved estimation methods, including more detailed information on the variability of river properties (~~such as channel~~i.e. depth and width~~), and~~). Future works should also relate the frequency of ~~hurricanes and tropical cyclones~~inundation depths to return periods of precipitation, river flows, and surges, as well as differentiate among the individual effects of the components to determine the role of each in flooding impact. This can be a very useful piece of information for deciding whether and where to take measures in terms of flood occurrence and the potential relocation of CI to avoid catastrophic compound flood events.

Notwithstanding these challenges, the findings of this study highlight that, whenever possible, risk assessments across different critical locations directly or indirectly affecting critical infrastructure should be based on a consistent set of compound risks. ~~Critical infrastructure is usually positioned by following the FEMA 100-year flood zone map. The areas outside the map are without mitigation plans and stand without any protection, on the other hand, these plans are based on some certain flood depth. In this study, however, we see an increase in flooded areas in the futuristic scenarios, as well as some under- and overestimation from the FEMA map, and that the flood depth at a location can essentially increase during a compound flooding. This may bring us to the conclusion that compound flooding extends the areas to be included in mitigation plans.~~

The proposed analysis suggests planning and management strategies for critical infrastructure should rely on historical flooding data, together with future storm scenarios and climate and SLR projections. The overall impact on each critical structure in terms of flood extent and depth is unique. This will ultimately allow the building of resilience into different components of critical infrastructure to enable the system to function even under disaster conditions or to recover more quickly.

~~Acknowledgements~~Acknowledgments: This work was supported by Eversource Energy.

Author contributions: MKh, GS, XS, EA conceived the study. XS and EA contributed to the conception of the hydrologic model. RL contributed to the production and analysis of the hydrologic model outputs. MKo and EN contributed to the analysis, and interpretation of the climatic data. MKh and GS contributed to the automation of the hydraulic model and the interpretation of its results. All authors participated in drafting the article and revising it critically for important intellectual content. All authors give the final approval of the published version.

Competing interests. The authors declare that they have no conflict of interest.

References

Abi-Samra, N. and Henry, W.: Actions Before and After a Flood – Substation Protection and Recovery from Weather Related Water Damage, IEEE Power & Energy Magazine, pp. 52–58, Mar/Apr. 2011.

Ahearn E.A., (2004). Scientific Investigations Report 2004-5160, https://doi.org/10.3133/sir20045160

Barnard, P. L., Erikson, L. H., Foxgrover, A. C., Hart, J. A. F., Limber, P., O'Neill, A. C., … Jones, J. M.: Dynamic flood modeling essential to assess the coastal impacts of climate change. Scientific Reports, 9(1), 4309. https://doi.org/10.1038/s41598-019-40742-z, 2019.

Barnard, P. L., Hoover, D., Hubbard, D. M., Snyder, A., Ludka, B. C., Allan, J., Kaminsky, G. M., Ruggiero, P., Gallien, T. W., Gabel, L., McCandless, D., Weiner, H. M., Cohn, N., Anderson, D. L. and Serafin, K. A.: Extreme oceanographic forcing and coastal response due to the 2015–2016 El Niño, Nat. Commun., 8(1), 14365, doi:10.1038/ncomms14365, 2017.

Bates, P. D., Dawson, R. J., Hall, J. W., Horritt, M. S., Nicholls, R. J., Wicks, J., & Hassan, M. A. A. M. (2005). Coastal Engineering, 52, 793–810.

Bevacqua, E., Maraun, D., Vousdoukas, M. I., Voukouvalas, E., Vrac, M., Mentaschi, L., Widmann, M.: Higher probability of compound flooding from precipitation and storm surgein Europe under anthropogenic climate change. Sci. Adv. 5, eaaw5531, 2019.

Blöschl, G., Hall, J., Parajka, J., Perdigão, R. A. P., Merz, B., Arheimer, B., Aronica, G. T., Bilibashi, A., Bonacci, O., Borga, M., Čanjevac, I., Castellarin, A., Chirico, G. B., Claps, P., Fiala, K., Frolova, N., Gorbachova, L., Gül, A., Hannaford, J., Harrigan, S., Kireeva, M., Kiss, A., Kjeldsen, T. R., Kohnová, S., Koskela, J. J., Ledvinka, O., Macdonald, N., Mavrova-Guirguinova, M., Mediero, L., Merz, R., Molnar, P., Montanari, A., Murphy, C., Osuch, M., Ovcharuk, V., Radevski, I., Rogger, M., Salinas, J. L., Sauquet, E., Šraj, M., Szolgay, J., Viglione, A., Volpi, E., Wilson, D., Zaimi, K. and Živković, N.: Changing climate shifts timing of European floods, Science (80-.)., 357(6351), 588–590, doi:10.1126/science.aan2506, 2017.

Bradbrook, K., Lane, S., Waller, S. and Bates, P.: Two-dimensional diffusion wave modelling of flood inundation using a simplified channel representation, Int. J. River Basin Manag., 2, 211–223 [online] Available from: https://research-information.bris.ac.uk/en/publications/two-dimensional-diffusion-wave-modelling-of-flood-inundation-usin (Accessed 13 October 2020), 2004.

Bunya, S., Dietrich, J. C., Westerink, J. J., Ebersole, B. A., Smith, J. M., Atkinson, J. H., … Roberts, H. J.: A High-Resolution Coupled Riverine Flow, Tide, Wind, Wind Wave, and Storm Surge Model for Southern Louisiana and Mississippi. Part I: Model Development and Validation. Monthly Weather Review, 138(2), 345–377. https://doi.org/10.1175/2009MWR2906.1, 2010.

Cañizares, R., & Irish, J. L.: Simulation of storm-induced barrier island morphodynamics and flooding. Coastal Engineering, 55(12), 1089–1101. https://doi.org/10.1016/J.COASTALENG.2008.04.006, 2008.

Cariolet, J.-M.: Use of high water marks and eyewitness accounts to delineate flooded coastal areas: The case of Storm Johanna (10 March 2008) in Brittany, France. Ocean & Coastal Management, 53(11), 679–690. https://doi.org/10.1016/J.OCECOAMAN.2010.09.002, 2010.

Chang, S. E., McDaniels, T. L., Mikawoz, J., Peterson, K.: Infrastructure failure interdependencies in extreme events: power outage consequences in the 1998 Ice Storm. Nat Hazards 41:337–358. doi: 10.1007/s11069-006-9039-4, 2007. Chang, S. E., McDaniels, T. L., Mikawoz, J., & Peterson, K.: Infrastructure failure interdependencies in extreme events: power outage consequences in the 1998 Ice Storm. Natural Hazards, 41(2), 337–358. https://doi.org/10.1007/s11069-006-9039-4, 2007.

Chou M.-D., and Suarez, M. J.: An efficient thermal infrared radiation parameterization for use in general circulation models. NASA Tech. Memo. 104606, 3, 85pp, 1994.

Cook A., Merwade, V., (2009) Effect of topographic data, geometric configuration and modeling approach on flood inundation mapping. Journal of Hydrology, 377, 1–2, 20, 131-142 https://doi.org/10.1016/j.jhydrol.2009.08.015

CtECO, C. E. C. O.: 2012 Impervious Surface Download, http://www.cteco.uconn.edu/projects/ms4/impervious2012.htm, 2012.

CtECO.: Connecticut Elevation (Lidar) Data, http://www.cteco.uconn.edu/data/lidar/index.htm, 2016.

D.A. Reed, M.D. Powell and J.M. Westerman, “Energy Supply System Performance for Hurricane Katrina,” Journal of Energy Engineering, pp. 95–102, Dec. 2010.

Danielson, J.J. and Gesch, D.B.: Global multi-resolution terrain elevation data 2010 (GMTED2010) (p. 26). US Department of the Interior, US Geological Survey, 2016.

Dawson, R. J., Thompson, D., Johns, D., Wood, R., Darch, G., Chapman, L., Hughes, P. N., Watson, G. V. R., Paulson, K., Bell, S., Gosling, S. N., Powrie, W. and Hall, J. W.: A systems framework for national assessment of climate risks to infrastructure, Philos. Trans. R. Soc. A Math. Phys. Eng. Sci., 376(2121), doi:10.1098/rsta.2017.0298, 2018.

de Bruijn, K., Buurman, J., Mens, M., Dahm, R. and Klijn, F.: Resilience in practice: Five principles to enable societies to cope with extreme weather events, Environ. Sci. Policy, 70, 21–30, doi:10.1016/j.envsci.2017.02.001, 2017. de Bruijn, K. M., Maran, C., Zygnerski, M., Jurado, J., Burzel, A., Jeuken, C. and Obeysekera, J.: Flood resilience of critical infrastructure: Approach and method applied to Fort Lauderdale, Florida, Water (Switzerland), 11(3), doi:10.3390/w11030517, 2019.

de Bruijn, K., Buurman, J., Mens, M., Dahm, R. and Klijn, F.: Resilience in practice: Five principles to enable societies to cope with extreme weather events, Environ. Sci. Policy, 70, 21–30, doi:10.1016/j.envsci.2017.02.001, 2017.

Dee, D.P., Uppala, S.M., Simmons, A.J., Berrisford, P., Poli, P., Kobayashi, S., Andrae, U., Balmaseda, M.A., Balsamo, G., Bauer, P., Bechtold, P., Beljaars, A.C.M., van de Berg, L., Bidlot, J., Bormann, N., Delsol, C., Dragani, R., Fuentes, M., Geer, A.J., Haimberger, L., Healy, S.B., Hersbach, H., Hólm, E.V., Isaksen, L., Kållberg, P., Köhler, M., Matricardi, M., McNally, A.P., Monge-Sanz, B.M., Morcrette, J.-J., Park, B.-K., Peubey, C., de Rosnay, P., Tavolato, C., Thépaut, J.-N. and Vitart, F.: The ERA-Interim reanalysis: Configuration and performance of the data assimilation system. Quart. J. Roy. Meteor. Soc., 137, 553–597, doi: https://doi.org/10.1002/qj.828, 2011.

Dottori, F., Szewczyk, W., Ciscar, J. C., Zhao, F., Alfieri, L., Hirabayashi, Y., Bianchi, A., Mongelli, I., Frieler, K., Betts, R. A. and Feyen, L.: Increased human and economic losses from river flooding with anthropogenic warming, Nat. Clim. Chang., 8(9), 781–786, doi:10.1038/s41558-018-0257-z, 2018.

FAO.: The digitized soil map of the world, World Soil Resource Rep. 67, FAO, Rome. FAO-UNESCO (1971–1981), Soil Map of the World (1:5,000,000), vol. 1–10, UNESCO, Paris, France. FAO-UNESCO (1974), Soil Map of the World (1:5,000,000), vol. 1 legend, UNESCO, Paris, France, 1991.

FEMA, CT DEEP (2013). Coastal Hazards Map Viewer Information http://www.cteco.uconn.edu/viewers/coastalhazards.htm#surge

FEMA.: Reducing Flood Effects in Critical Facilities. HSFE60-13-(April), 1–11, 2013.

~~Friedl, M., Sulla-Menashe, D.: MCD12Q1 MODIS/Terra+Aqua Land Cover Type Yearly L3 Global 500m SIN Grid V006. NASA EOSDIS Land Processes DAAC. https://doi.org/10.5067/MODIS/MCD12Q1.006, 2015.~~

Friedl M. A., Sulla-Menashe D., Tan B., Schneider A., Ramankutty N., Sibley A., & Huang X.: MODIS Collection 5 global land cover: Algorithm refinements and characterization of new datasets. Remote Sensing of Environment, 114(1), 168 10.1016/j.rse.2009.08.016–182), 2010.

Friedl, M., Sulla-Menashe, D.: MCD12Q1 MODIS/Terra+Aqua Land Cover Type Yearly L3 Global 500m SIN Grid V006. NASA EOSDIS Land Processes DAAC. https://doi.org/10.5067/MODIS/MCD12Q1.006, 2015.

Gerald, A. M., Covey, C, Delworth, T., Latif, M., McAvaney, B., Mitchell, J. F. B., Stouffer, R. J., and Taylor, K. E.: The WCRP CMIP3 multimodel dataset: A new era in climate change research. Bulletine of American Meteorological Society, 2007.

Grell, G. A., and Dévényi, D., A generalized approach to parameterizing convection combining ensemble and data assimilation techniques, Geophys. Res. Lett., 29(14), doi:10.1029/2002GL015311, 2002.

Hallegatte, S., Green, C., Nicholls, R. J., Corfee-Morlot, J.: Future flood losses in major coastal cities. Nat Clim Chang 3:802–806. doi: 10.1038/nclimate1979, 2013.

Hamman, J. J., Hamlet, A. F., Lee, S.-Y., Fuller, R. and Grossman, E. E.: Combined Effects of Projected Sea Level Rise, Storm Surge, and Peak River Flows on Water Levels in the Skagit Floodplain, Northwest Sci., 90(1), 57–78, doi:10.3955/046.090.0106, 2016.

Hamman, J. J., Hamlet, A. F., Lee, S.-Y., Fuller, R., & Grossman, E. E.: Combined Effects of Projected Sea Level Rise, Storm Surge, and Peak River Flows on Water Levels in the Skagit Floodplain. Northwest Science, 90(1), 57–78. https://doi.org/10.3955/046.090.0106, 2016.

Hardesty, S., Shen, X., Nikolopoulos, E., & Anagnostou, E.: A Numerical Framework for Evaluating Flood Inundation Hazard under Different Dam Operation Scenarios—A Case Study in Naugatuck River. Water, 10(12), 1798. https://doi.org/10.3390/w10121798, 2018.

Higgins, R.W.: Climate Prediction Center (U.S.).S). Improved United States Precipitation Quality Control System and Analysis; NCEP/Climate Prediction Center Atlas, NOAA, National Weather Service, National Centers for Environmental Prediction, Climate Prediction Center: Camp Springs, MD, USA, 2000.

Hostache, R., Matgen, P., Schumann, G., Puech, C., Hoffmann, L., & Pfister, L.: Water Level Estimation and Reduction of Hydraulic Model Calibration Uncertainties Using Satellite SAR Images of Floods. IEEE Transactions on Geoscience and Remote Sensing, 47(2), 431–441. https://doi.org/10.1109/TGRS.2008.2008718, 2009.

Jordi, A., Georgas, N., Blumberg, A., Yin, L., Chen, Z., Wang, Y., Schulte, J., Ramaswamy, V., Runnels, D. and Saleh, F.: A next-generation coastal ocean operational system, Bull. Am. Meteorol. Soc., 100(1), 41–53, doi:10.1175/BAMS-D-17-0309.1, 2019.

Karagiannis, G.M., Chondrogiannis, S., Krausmann, E. and Turksezer, Z.I.: Power grid recovery after natural hazard impact. Science for Policy report by the Joint Research Centre (JRC), European Union. https://doi.org/10.2760/87402, 2017.

Koenig, T.A., Bruce, J.L., O'Connor, J.E., McGee, B.D., Holmes, R.R., Jr., Hollins, Ryan, Forbes, B.T., Kohn, M.S., Schellekens, M.F., Martin, Z.W., and Peppler, M.C.: Identifying and preserving high-water mark data: U.S.S Geological Survey Techniques and Methods, book 3, chap. A24, 47 p., http://dx.doi.org/10.3133/tm3A24, 2016.

Kwasinski, W.W. Weaver, P.L. Chapman and P.T. Krein, "Telecommunications Power Plant Damage Assessment for Hurricane Katrina – Site Survey and Follow-Up Results," IEEE Systems Journal, vol. 3, no. 3, pp. 277–287, Nov. 2009.

Lackmann, G. M.: Hurricane Sandy before 1900, and after 2100. Bull. Amer. 699 Meteor. Soc., 96, 547-560, doi: 10.1175/BAMS-D-14-00123.1, 2015.

Leonard, M., Westra, S., Phatak, A., Lambert, M., Van Den Hurk, B., Mcinnes, K., … Stafford-Smith, M.: A compound event framework for understanding extreme impacts. WIREs Clim Change, 5, 113–128. https://doi.org/10.1002/wcc.252, 2014.

Lin, N., Kopp, R. E., Horton, B. P., & Donnelly, J. P.: Hurricane Sandy's flood frequency increasing from year 1800 to 2100. Proceedings of the National Academy of Sciences of the United States of America, 113(43), 12071–12075. https://doi.org/10.1073/pnas.1604386113, 2016.

Marsooli, R., Lin, N., Emanuel, K., & Feng, K.: Climate change exacerbates hurricane flood hazards along US Atlantic and Gulf Coasts in spatially varying patterns. Nature Communications, 10(1). https://doi.org/10.1038/s41467-019-11755-z, 2019.

McEvoy, D., Ahmed, I., Mullett, J.: The impact of the 2009 heat wave on Melbourne's critical infrastructure. Local Environ 17:783–796. doi: 10.1080/13549839.2012.678320, 2012.

Meehl, G. A., C. Covey, K. E. Taylor, T. Delworth, R. J. Stouffer, M. Latif, B. McAvaney, and J. F. B. Mitchell: The WCRP CMIP3 multimodel dataset: A new era in climate change research. Bull. Amer. Meteor, 2007.

Mlawer, E. J., Taubman, S. J., Brown, P. D., Iacono, M. J. and Clough, S. A.: Radiative transfer for inhomogeneous atmospheres: RRTM, a validated correlated–k model for the longwave. J. Geophys. Res., 102, 16663–16682. doi:10.1029/97JD00237, 1997.

Moftakhari, H. R., Salvadori, G., AghaKouchak, A., Sanders, B. F., & Matthew, R. A.: Compounding effects of sea level rise and fluvial flooding. Proceedings of the National Academy of Sciences of the United States of America, 114(37), 9785–9790. https://doi.org/10.1073/pnas.1620325114, 2017.

Muis, S., Verlaan, M., Winsemius, H. C., Aerts, J. C. J. H. and Ward, P. J.: A global reanalysis of storm surges and extreme sea levels, Nat. Commun., 7, doi:10.1038/ncomms11969, 2016.

NOAA.: NOAA's STATE OF THE COAST: National Coastal Population Report, 2013.

O'Donnell, J.: Sea Level Rise Connecticut Final Report. https://circa.uconn.edu/wp-content/uploads/sites/1618/2019/02/SeaLevelRiseConnecticut-Final-Report.pdf, 2017. (last accessed January 10, 2020)

Pant, R., Thacker, S., Hall, J. W., Alderson, D. and Barr, S.: Critical infrastructure impact assessment due to flood exposure, J. Flood Risk Manag., 11(1), 22–33, doi:10.1111/jfr3.12288, 2018.

Pasquier, U., He, Y., Hooton, S., Goulden, M. and Hiscock, K. M.: An integrated 1D–2D hydraulic modelling approach to assess the sensitivity of a coastal region to compound flooding hazard under climate change, Nat. Hazards, 98(3), 915–937, doi:10.1007/s11069-018-3462-1, 2019.

Pearson, J., Punzo, G., Mayfield, M., Brighty, G., Parsons, A., Collins, P., Jeavons, S. and Tagg, A.: Flood resilience: consolidating knowledge between and within critical infrastructure sectors, Environ. Syst. Decis., 38(3), 318–329, doi:10.1007/s10669-018-9709-2, 2018.

Powers, J. G., Klemp, J. B., Skamarock, W. C., Davis, C. A., Dudhia, J., Gill, D. O., Coen, J. L. and Gochis, D. J.: The Weather Research and Forecasting Model: Overview, system efforts, and future directions. Bull. Amer. Meteor. Soc., 98, 1717 1737, https://doi.org/10.1175/BAMS-D-15-00308.1, 2017.

Quinn, N., Bates, P. D., Neal, J., Smith, A., Wing, O., Sampson, C., Smith, J. and Heffernan, J.: The Spatial Dependence of Flood Hazard and Risk in the United States, Water Resour. Res., 55(3), 1890–1911, doi:10.1029/2018WR024205, 2019.

Schumann, G., Hostache, R., Puech, C., Hoffmann, L., Matgen, P., Pappenberger, F., & Pfister, L.: High-Resolution 3-D Flood Information From Radar Imagery for Flood Hazard Management. IEEE Transactions on Geoscience and Remote Sensing, 45(6), 1715–1725. https://doi.org/10.1109/TGRS.2006.888103, 2007.

Schumann, G., Matgen, P., Cutler, M. E. J., Black, A., Hoffmann, L., & Pfister, L.: Comparison of remotely sensed water stages from LiDAR, topographic contours and SRTM. ISPRS Journal of Photogrammetry and Remote Sensing, 63(3), 283–296. https://doi.org/10.1016/J.ISPRSJPRS.2007.09.004, 2008.

Schumann, G., Matgen, P., Hoffmann, L., Hostache, R., Pappenberger, F., & Pfister, L.: Deriving distributed roughness values from satellite radar data for flood inundation modelling. Journal of Hydrology, 344(1–2), 96–111. https://doi.org/10.1016/J.JHYDROL.2007.06.024, 2007.

Shen, X., & Anagnostou, E. N.: A framework to improve hyper-resolution hydrological simulation in snow-affected regions. Journal of Hydrology, 552, 1–12. https://doi.org/10.1016/j.jhydrol.2017.05.048, 2017.

Skamarock, W. C., Klemp, J. B., Dudhia, J., Gill, D. O., Barker, D. M., Duda, M. G., Huang, X., Wang, W. and Powers, J. G.: A description of the Advanced Research WRF version 3. NCAR Tech. Note NCAR/TN-475+STR, 113 pp., https://doi .org/10.5065/D68S4MVH, 2008.

Song–You, H., Noh, Y. and Dudhia, J.: A new vertical diffusion package with an explicit treatment of entrainment processes. Mon. Wea. Rev., 134, 2318 2341. doi:10.1175/MWR3199.1, 2006.

Székely, G. J., Rizzo, M. L. and Bakirov, N. K.: MEASURING AND TESTING DEPENDENCE BY CORRELATION OF DISTANCES, Ann. Stat., 35(6), 2769–2794, doi:10.1214/009053607000000505, 2007.

Tewari, M.F., Chen, W., Wang, J., Dudhia, M.A., LeMone, K., Mitchell, M.E., Gayno, G., Wegiel, J. and Cuenca, R.H.: Implementation and verification of the unified NOAH land surface model in the WRF model. 20th conference on weather analysis and forecasting/16th conference on numerical weather prediction, pp. 11–15, 2004.

Thompson, G., Paul, R. F., Roy, M. R. & William, D. H.: Explicit Forecasts of Winter Precipitation Using an Improved Bulk Microphysics Scheme. Part II: Implementation of a New Snow Parameterization. Mon. Wea. Rev., 136, 5095–5115. doi:10.1175/2008MWR2387.1, 2008.

U.S.S Geological Survey.: 1/9th Arc-second Digital Elevation Models (DEMs) - USGS National Map 3DEP Downloadable Data Collection: U.S.S Geological Survey., 2017.

Vousdoukas, M. I., Mentaschi, L., Voukouvalas, E., Verlaan, M., Jevrejeva, S., Jackson, L. P. and Feyen, L.: Global probabilistic projections of extreme sea levels show intensification of coastal flood hazard, Nat. Commun., 9(1), 1–12, doi:10.1038/s41467-018-04692-w, 2018.

Vousdoukas, M. I., Mentaschi, L., Voukouvalas, E., Verlaan, M., Jevrejeva, S., Jackson, L. P. and Feyen, L.: Global probabilistic projections of extreme sea levels show intensification of coastal flood hazard, Nat. Commun., 9(1), 1–12, doi:10.1038/s41467-018-04692-w, 2018.

Wahl, T., Jain, S., Bender, J., Meyers, S. D., & Luther, M. E.: Increasing risk of compound flooding from storm surge and rainfall for major US cities. Nature Climate Change, 5(12), 1093–1097. https://doi.org/10.1038/nclimate2736, 2015.

Wahl, T., Ward, P., Winsemius, H., AghaKouchak, A., Bender, J., Haigh, I., … Westra, S.: When Environmental Forces Collide. Eos, 99. https://doi.org/10.1029/2018EO099745, 2018.

Wang, H., Loftis, J., Liu, Z., Forrest, D. and Zhang, J.: The Storm Surge and Sub-Grid Inundation Modeling in New York City during Hurricane Sandy, J. Mar. Sci. Eng., 2(1), 226–246, doi:10.3390/jmse2010226, 2014.

Warner, N. N., & Tissot, P. E.: Storm flooding sensitivity to sea level rise for Galveston Bay, Texas. Ocean Engineering, 44, 23–32. https://doi.org/10.1016/J.OCEANENG.2012.01.011, 2012.

~~Vousdoukas, M. I., Mentaschi, L., Voukouvalas, E., Verlaan, M., Jevrejeva, S., Jackson, L. P. and Feyen, L.: Global probabilistic projections of extreme sea levels show intensification of coastal flood hazard, Nat. Commun., 9(1), 1–12, doi:10.1038/s41467-018-04692-w, 2018.~~

Winsemius, H. C., Van Beek, L. P. H., Jongman, B., Ward, P. J. and Bouwman, A.: A framework for global river flood risk assessments, Hydrol. Earth Syst. Sci, 17, 1871–1892, doi:10.5194/hess-17-1871-2013, 2013.

Xia, Y., Mitchell, K., Ek, M., Sheffield, J., Cosgrove, B., Wood, E., … Mocko, D. .: Continental-scale water and energy flux analysis and validation for the North American Land Data Assimilation System project phase 2 (NLDAS-

2): 1. Intercomparison and application of model products. Journal of Geophysical Research: Atmospheres, 117(D3), n/a-n/a. https://doi.org/10.1029/2011JD016048, 2012.

Xian, S., Lin, N. and Hatzikyriakou, A.: Storm surge damage to residential areas: a quantitative analysis for Hurricane Sandy in comparison with FEMA flood map, Nat. Hazards, 79(3), 1867–1888, doi:10.1007/s11069-015-1937-x, 2015.

Ziervogel, G., New, M., Archer van Garderen, E., Midgley, G., Taylor, A., Hamann, R., Stuart-Hill, S., Myers, J. and Warburton, M.: Climate change impacts and adaptation in South Africa. Wiley Interdiscip Rev Clim Chang 5:605–620. doi: 10.1002/wcc.295, 2014.

Ziervogel, G., New, M., Archer van Garderen, E., Midgley, G., Taylor, A., Hamann, R., … Warburton, M.: Climate change impacts and adaptation in South Africa. Wiley Interdisciplinary Reviews: Climate Change, 5(5), 605–620. https://doi.org/10.1002/wcc.295, 2014.

Zscheischler, J., Westra, S., van den Hurk, B. J. J. M., Seneviratne, S. I., Ward, P. J., Pitman, A., … Zhang, X.: Future climate risk from compound events. Nature Climate Change, 8(6), 469–477. https://doi.org/10.1038/s41558-018-0156-3, 2018.

~~Dee, D.P., Uppala, S.M., Simmons, A.J., Berrisford, P., Poli, P., Kobayashi, S., Andrae, U., Balmaseda, M.A., Balsamo, G., Bauer, P., Bechtold, P., Beljaars, A.C.M., van de Berg, L., Bidlot, J., Bormann, N., Delsol, C., Dragani, R., Fuentes, M., Geer, A.J., Haimberger, L., Healy, S.B., Hersbach, H., Hólm, E.V., Isaksen, L., Kållberg, P., Köhler, M., Matricardi, M., McNally, A.P., Monge-Sanz, B.M., Morcrette, J.-J., Park, B.-K., Peubey, C., de Rosnay, P., Tavolato, C., Thépaut, J.-N. and Vitart, F.: The ERA-Interim reanalysis: Configuration and performance of the data assimilation system. Quart. J. Roy. Meteor. Soc., 137, 553–597, doi: https://doi.org/10.1002/qj.828, 2011.~~

~~Meehl, G. A., C. Covey, K. E. Taylor, T. Delworth, R. J. Stouffer, M. Latif, B. McAvaney, and J. F. B. Mitchell: The WCRP CMIP3 multimodel dataset: A new era in climate change research. Bull. Amer. Meteor, 2007.~~

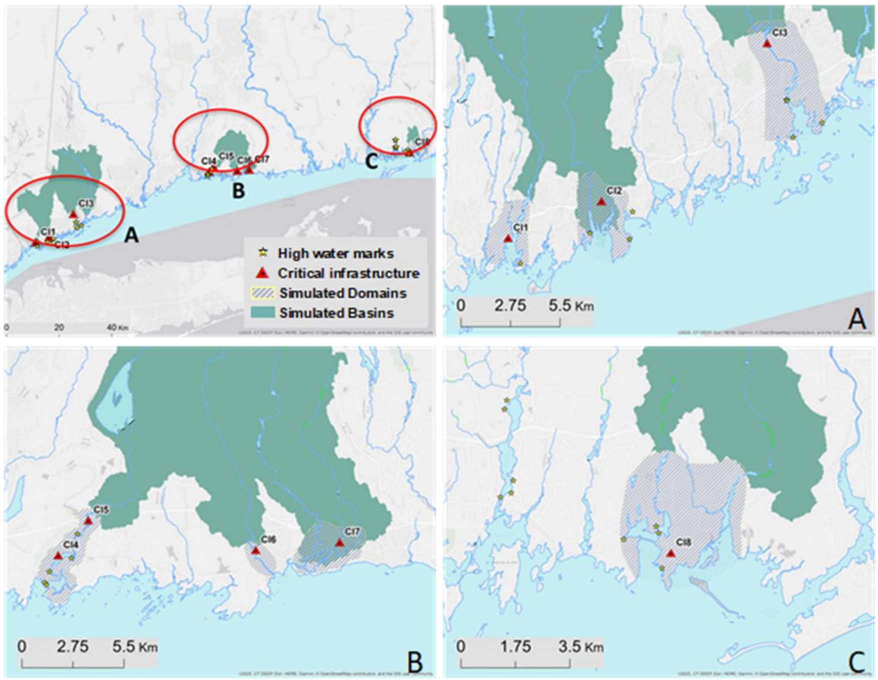

High water marks
Critical infrastructure
Simulated Domains
Simulated Basins
A
B
C
CI1
CI2
CI3
CI4
CI5
CI6
CI7
CI8
0 2.75 5.5 Km
0 1.75 3.5 Km

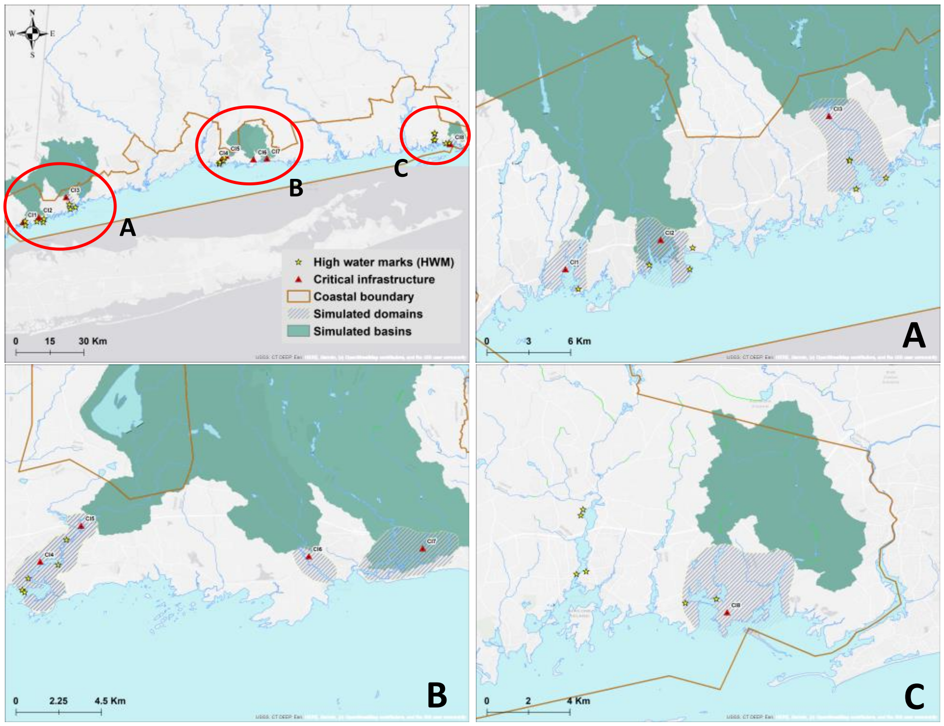

Figure 1: Study area with associated watersheds and simulation domains. Locations of substations and USGS high water marks ~~is~~are also shown. Red circles in the top left-hand panel, and marked with A, B, and C are highlighted in the panels A to C respectively. Background map by ESRI web-services, provided by UConn/CTDEEP, Esri, Garmin, USGS, NGA, EPA, USDA, NPS

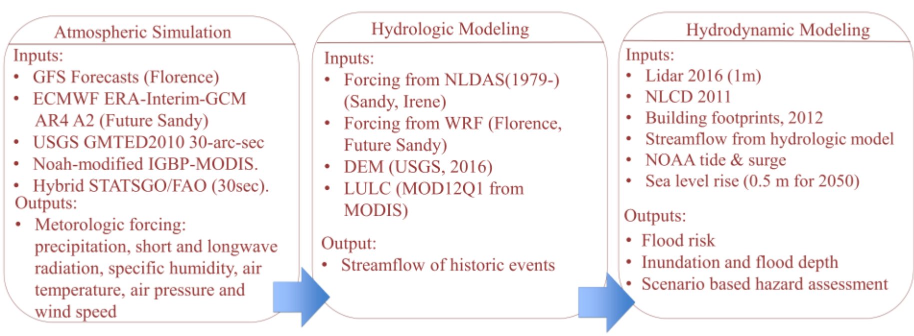

Figure 2: Considered framework including atmospheric simulations, hydrologic, and hydrodynamic modeling. Hurricane events (actual and simulated), and inputs and outputs of each component are shown. Readers should refer to chapter 2.2 for specifications

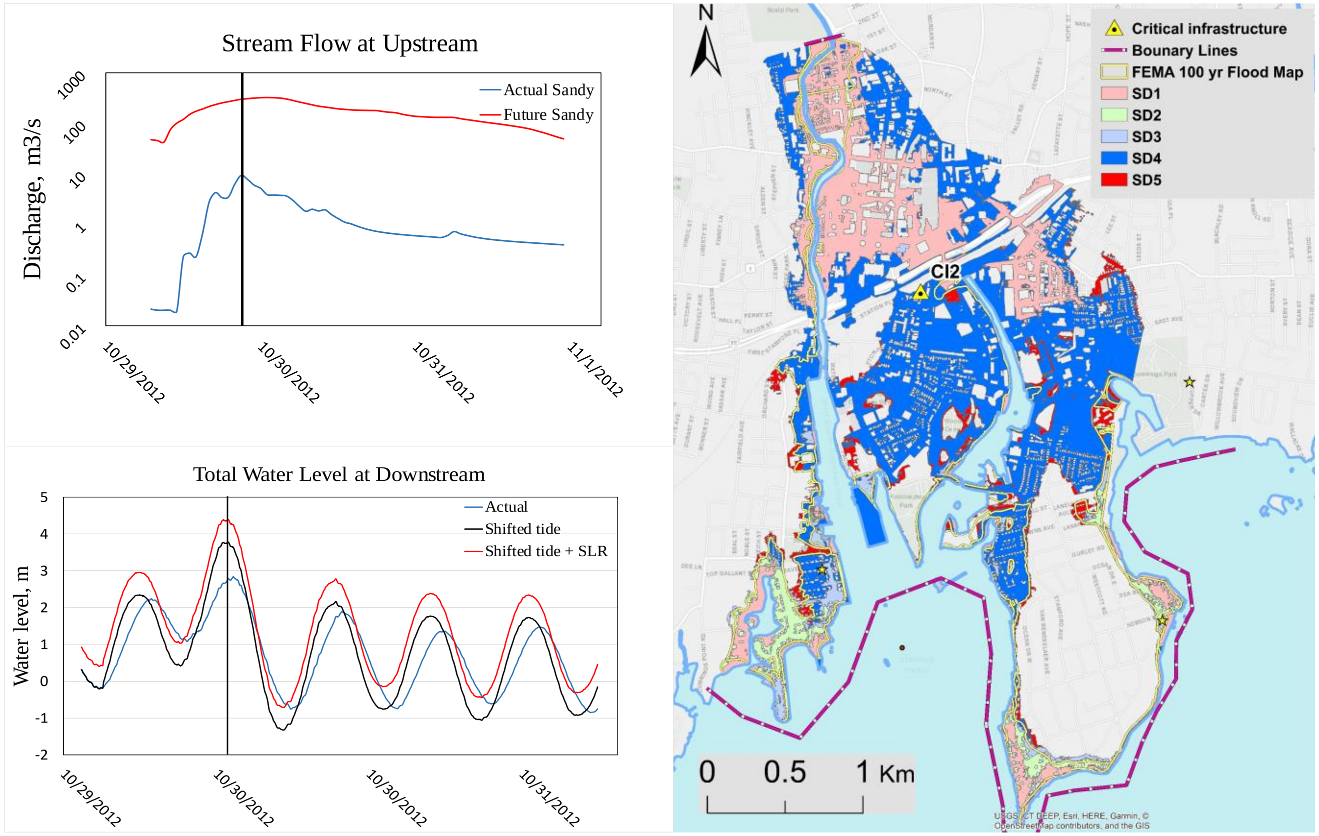

Figure 3: Example of different scenarios showing the upstream boundary condition (top left-hand panel, including the discharge for actual Sandy and future Sandy), and downstream boundary (bottom left-hand panel, including tide, shifted tide, and shifted tide with SLR). Output flood extend is also shown (right-hand panel), including results for SD1 to SD5 [reader should refer to Tab. 3 and chapter 2.2 for specification on the scenarios]). Background map on the firhg-hand panel by ESRI web-services, provided by UConn/CTDEEP, Esri, Garmin, USGS, NGA, EPA, USDA, NPS

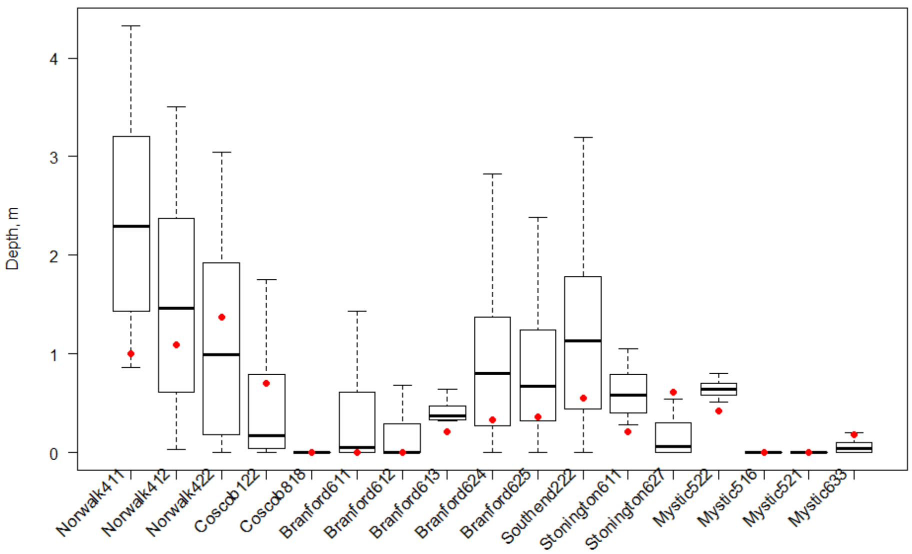
Depth, m
4
3
2
1
0
Norwalk411
Norwalk412
Norwalk422
Coscob122
Coscob818
Branford611
Branford612
Branford613
Branford624
Branford625
Southend222
Stonington611
Stonington627
Mystic522
Mystic516
Mystic521
Mystic633

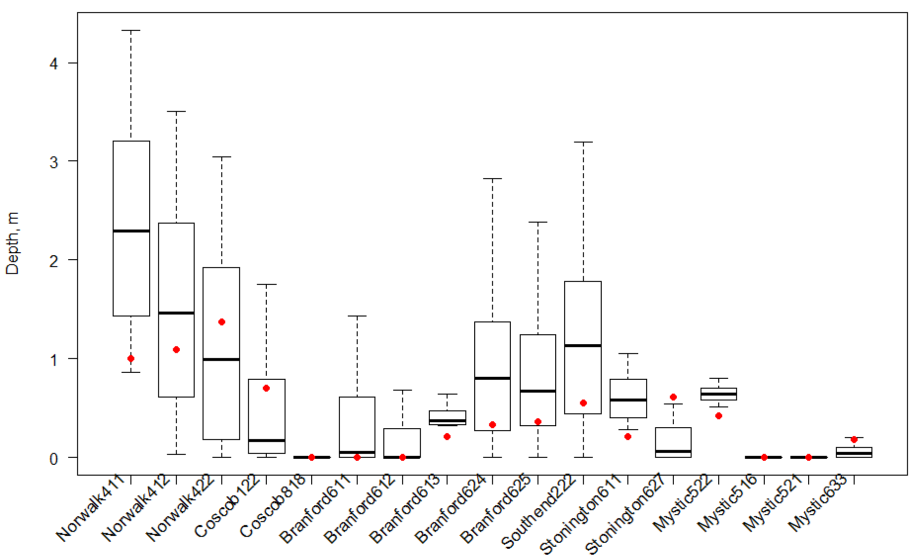
Depth, m
4
3
2
1
0
Norwalk411
Norwalk412
Norwalk422
Coscob122
Coscob818
Branford611
Branford612
Branford613
Branford624
Branford625
Southend222
Stonington611
Stonington627
Mystic522
Mystic516
Mystic521
Mystic633

Figure 4: Validation results (boxplot of water depth within 10x10m around the high-water mark -HWM- location) compared to selected HWM (red dots) by USGS

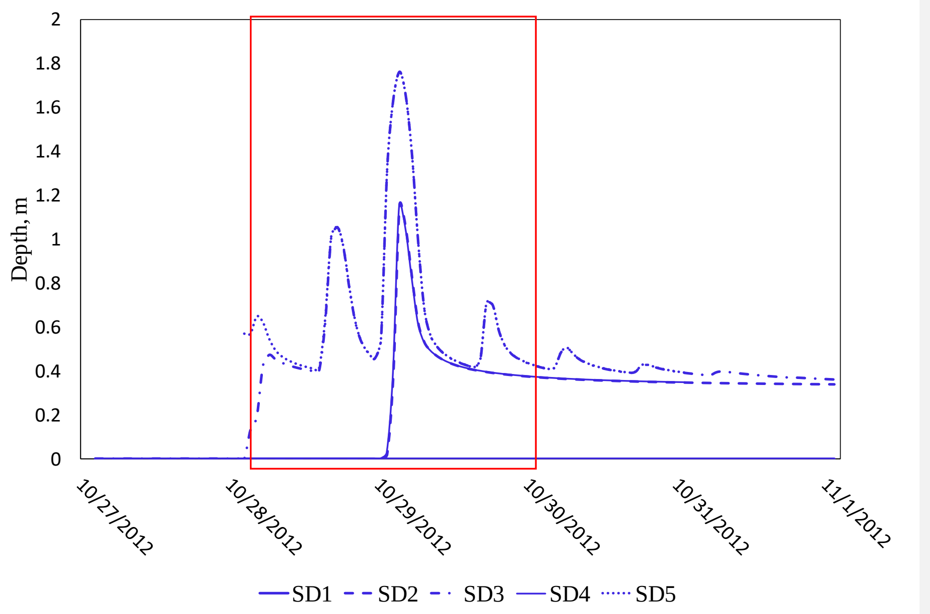

Depth, m
2
1.8
1.6
1.4
1.2
1
0.8
0.6
0.4
0.2
0
10/27/2012
10/28/2012
10/29/2012
10/30/2012
10/31/2012
11/1/2012
SD1
SD2
SD3
SD4
SD5

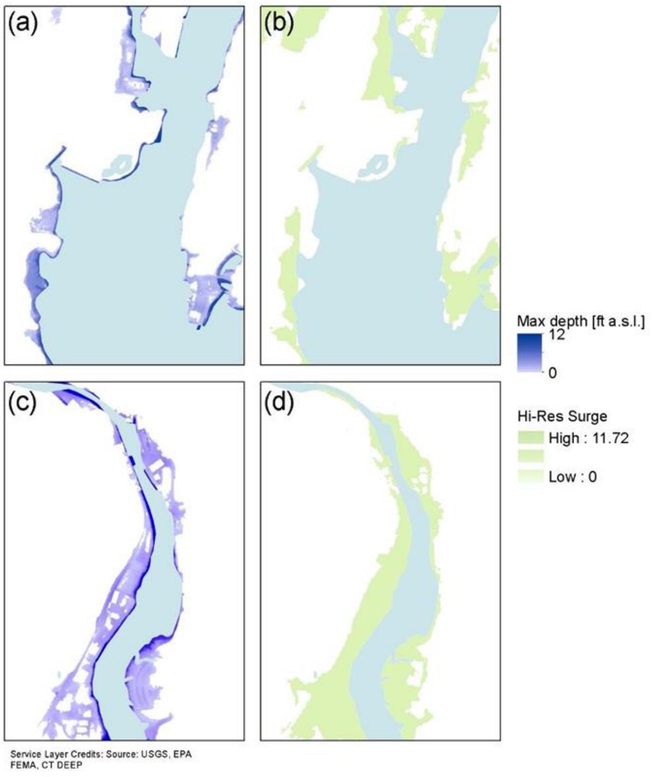

Figure 5: Comparison between the results of the proposed model for two selected locations (a,c, CI1 and CI2 respectively) and the maximum surge extent as proposed by CtEco (c,d respectively).

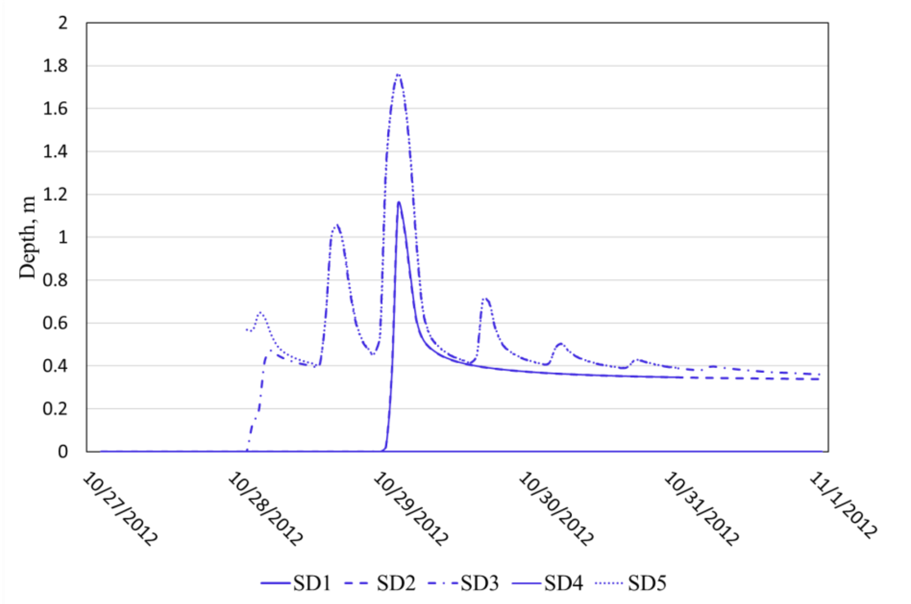

Figure 6: Example of time series of depth values for the different scenarios of Sandy event at CI3 [SD1 to SD5, readers should refer to Table 3 and chapter 2.24 for specification on the scenarios] ~~(Red rectangle shows the considered 24 hours window around the peak flow for calculation of the peak over threshold)~~

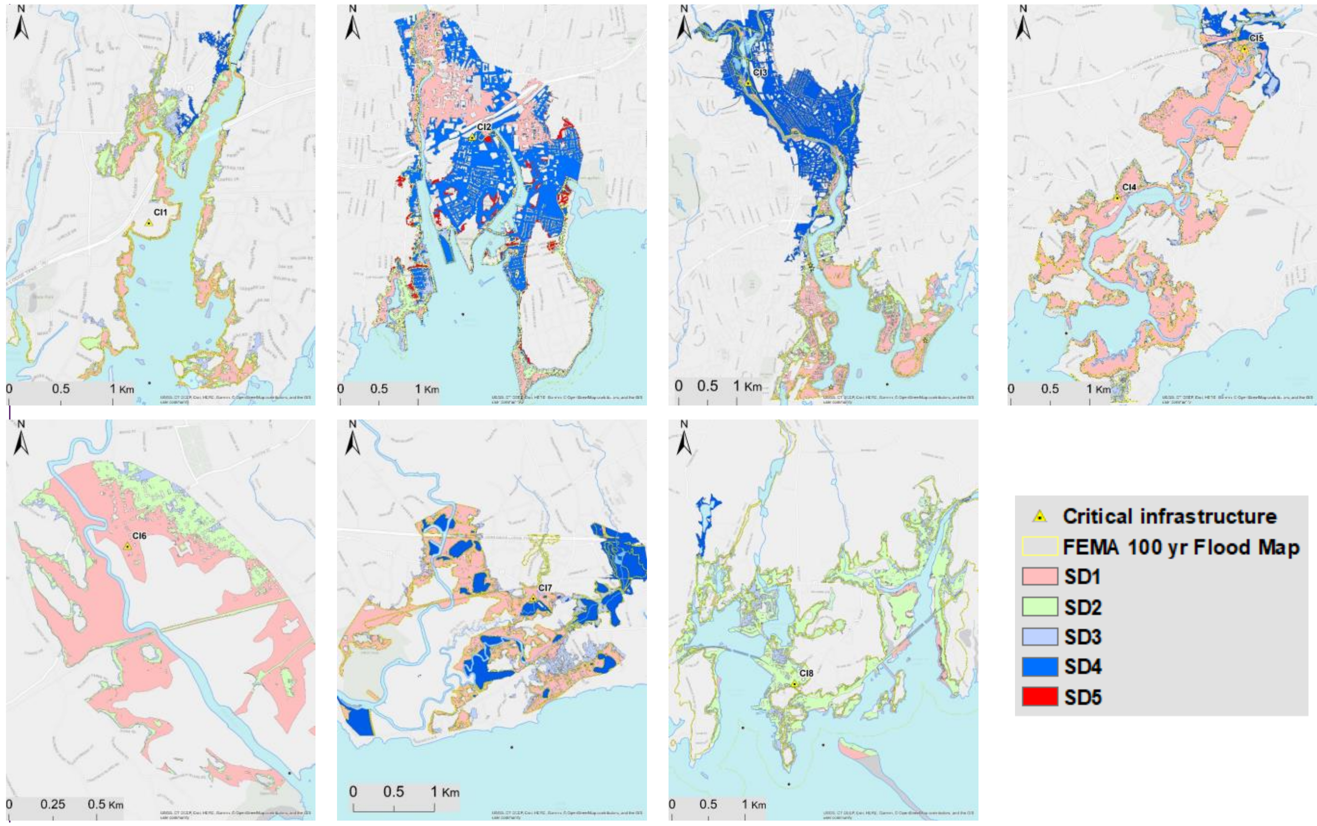

Figure 6a: Map overlay of maximum inundation for all the study domains containing CI1 through CI8 for the scenarios of Sandy [SD1 to SD5, readers should refer to Table 3 and chapter 2.2 for specification on the scenarios]

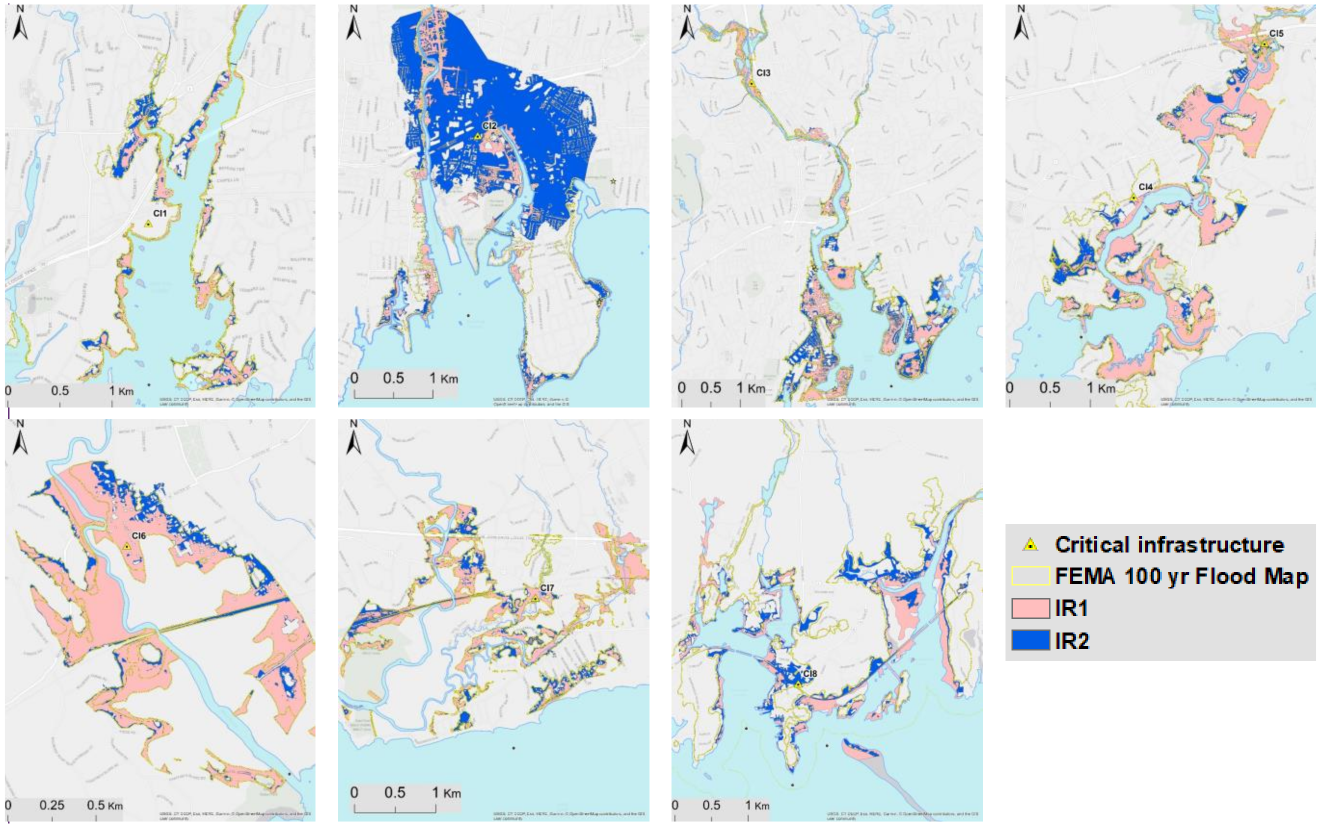

Figure 6b: Map overlay of maximum inundation for all the study domains containing CI1 through CI8 for the scenarios of Irene [IR1 and IR2, readers should refer to Tab. 3 and chapter 2.2 for specification on the scenarios]. Background map by ESRI web-services, provided by UConn/CTDEEP, Esri, Garmin, USGS, NGA, EPA, USDA, NPS

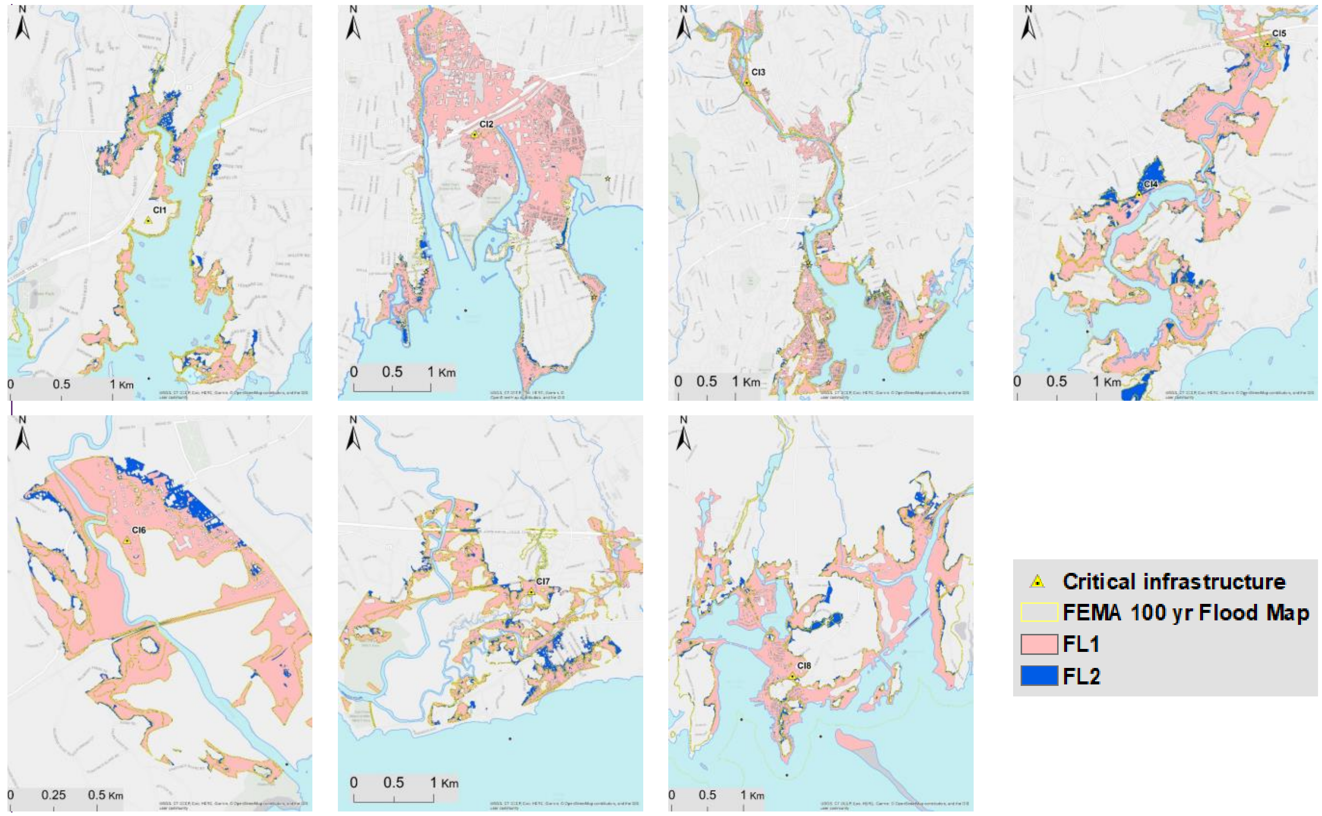

Figure 6c: Map overlay of maximum inundation for all the study domains containing CI1 through CI8 for the scenarios of Florence [FL1 and FL2, readers should refer to Table 3 and chapter 2.2 for specification on the scenarios]. Background map by ESRI web-services, provided by UConn/CTDEEP, Esri, Garmin, USGS, NGA, EPA, USDA, NPS

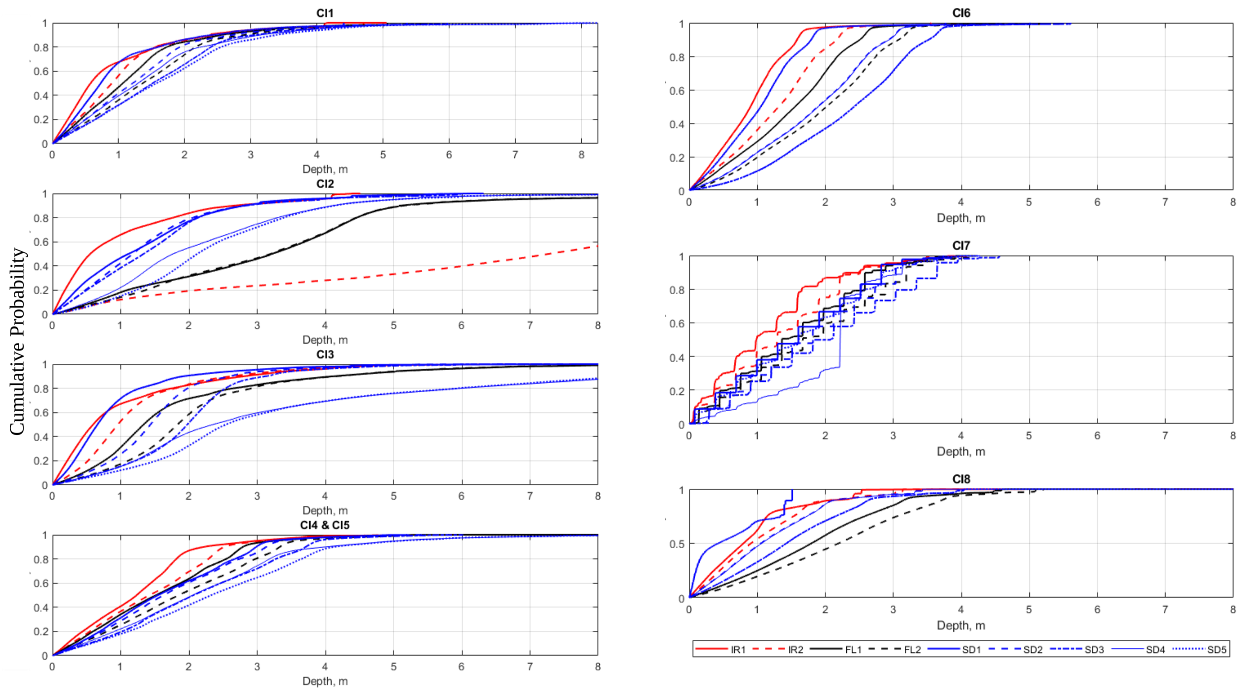

Figure 7: Cumulative density plot of the depth of all the flooded cells during maximum inundation. Hurricanes scenarios are labelled according to Table 3 and explained in chapter 2.2. Critical infrastructures are labelled CI1 to CI8, as described in Table 1.

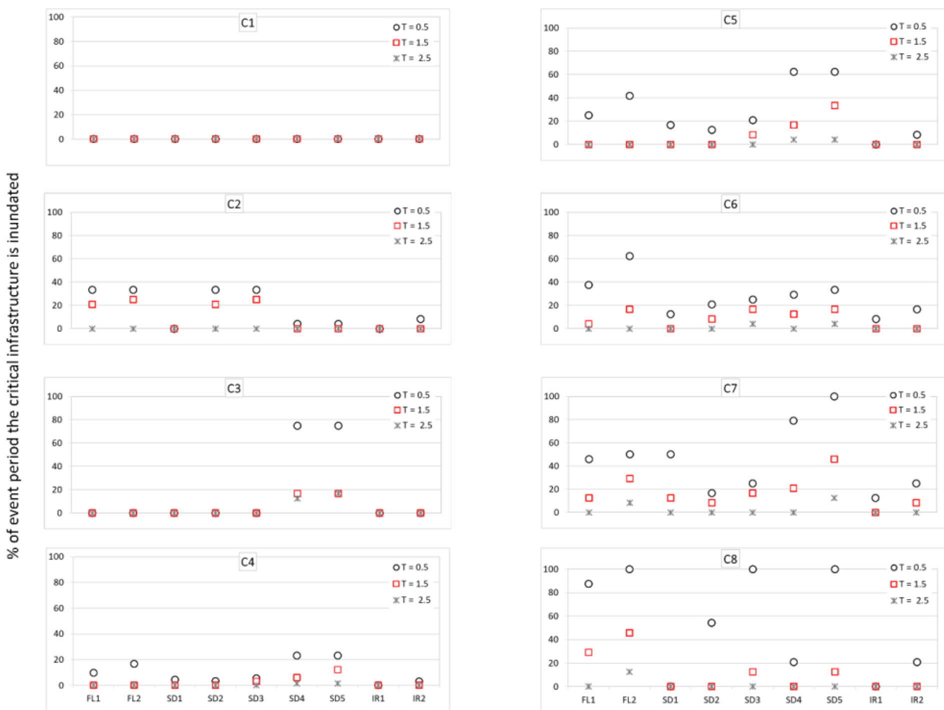

% of event period the critical infrastructure is inundated
C1
C2
C3
C4
C5
C6
C7
C8
T = 0.5
T = 1.5
T = 2.5
FL1
FL2
SD1
SD2
SD3
SD4
SD5
IR1
IR2

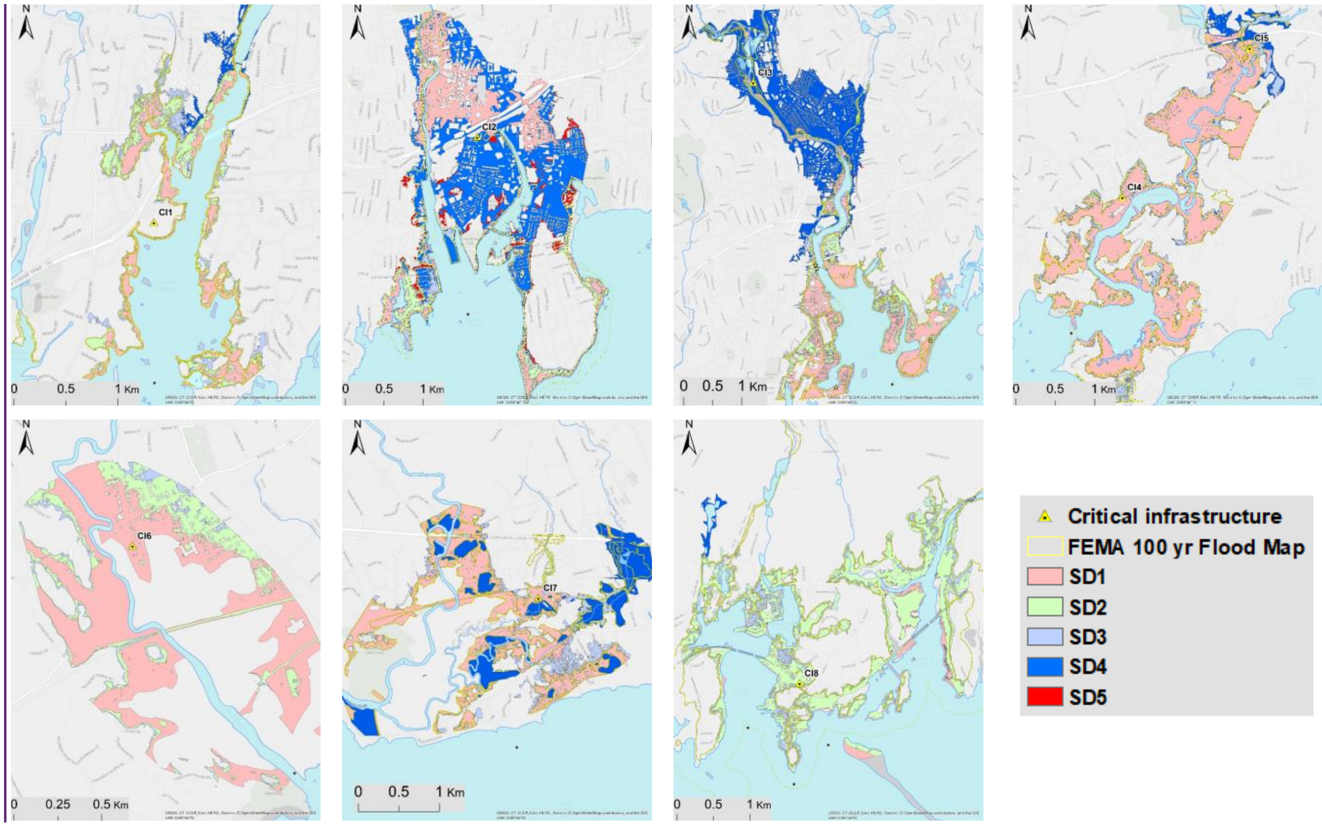

Figure 7a: Map overlay of maximum inundation for all the study domains containing CI1 through CI8 for the scenarios of Sandy [SD1 to SD5, readers should refer to Table 3 and chapter 2.2 for specification on the scenarios]

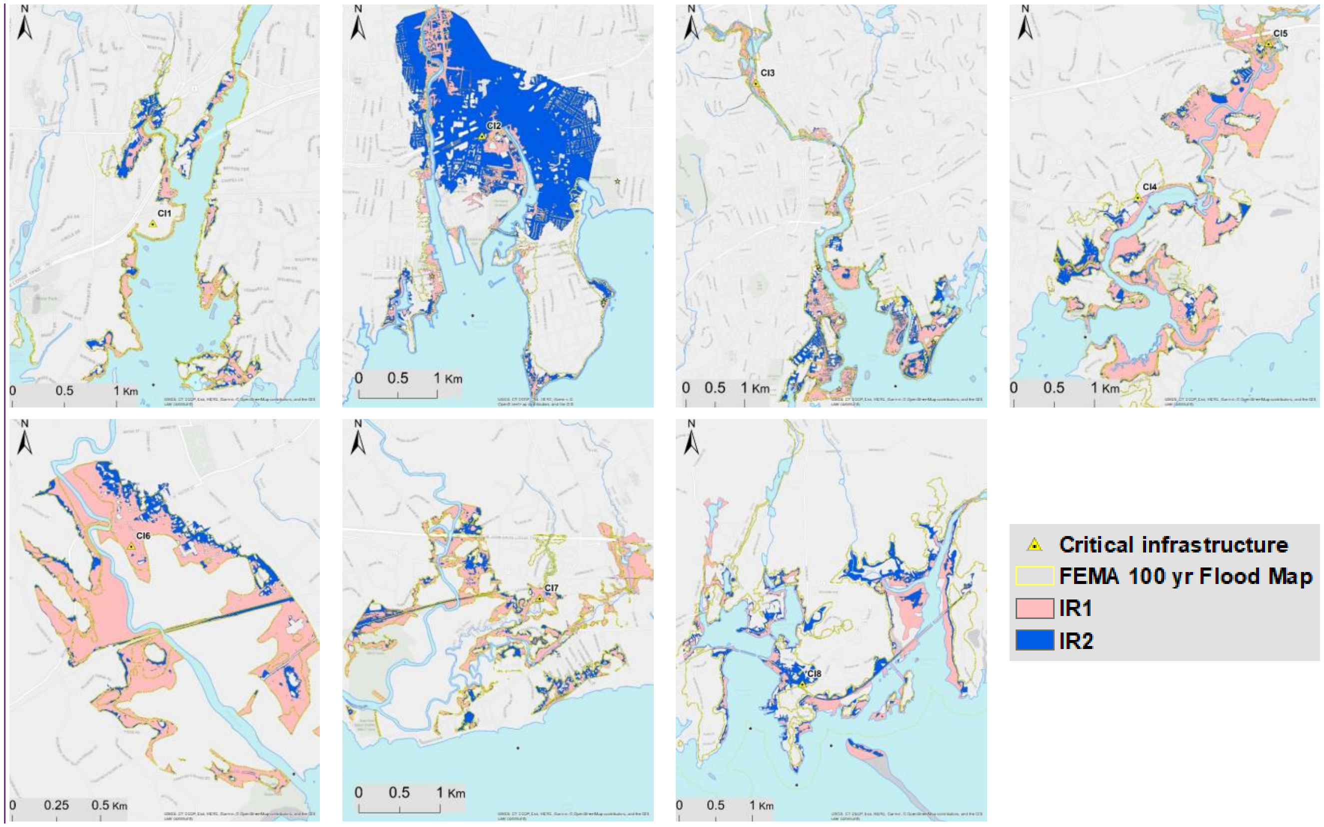

Figure 7b: Map overlay of maximum inundation for all the study domains containing CI1 through CI8 for the scenarios of Irene [IR1 and IR2, readers should refer to Tab. 3 and chapter 2.2 for specification on the scenarios]. Background map by ESRI web-services, provided by UConn/CTDEEP, Esri, Garmin, USGS, NGA, EPA, USDA, NPS

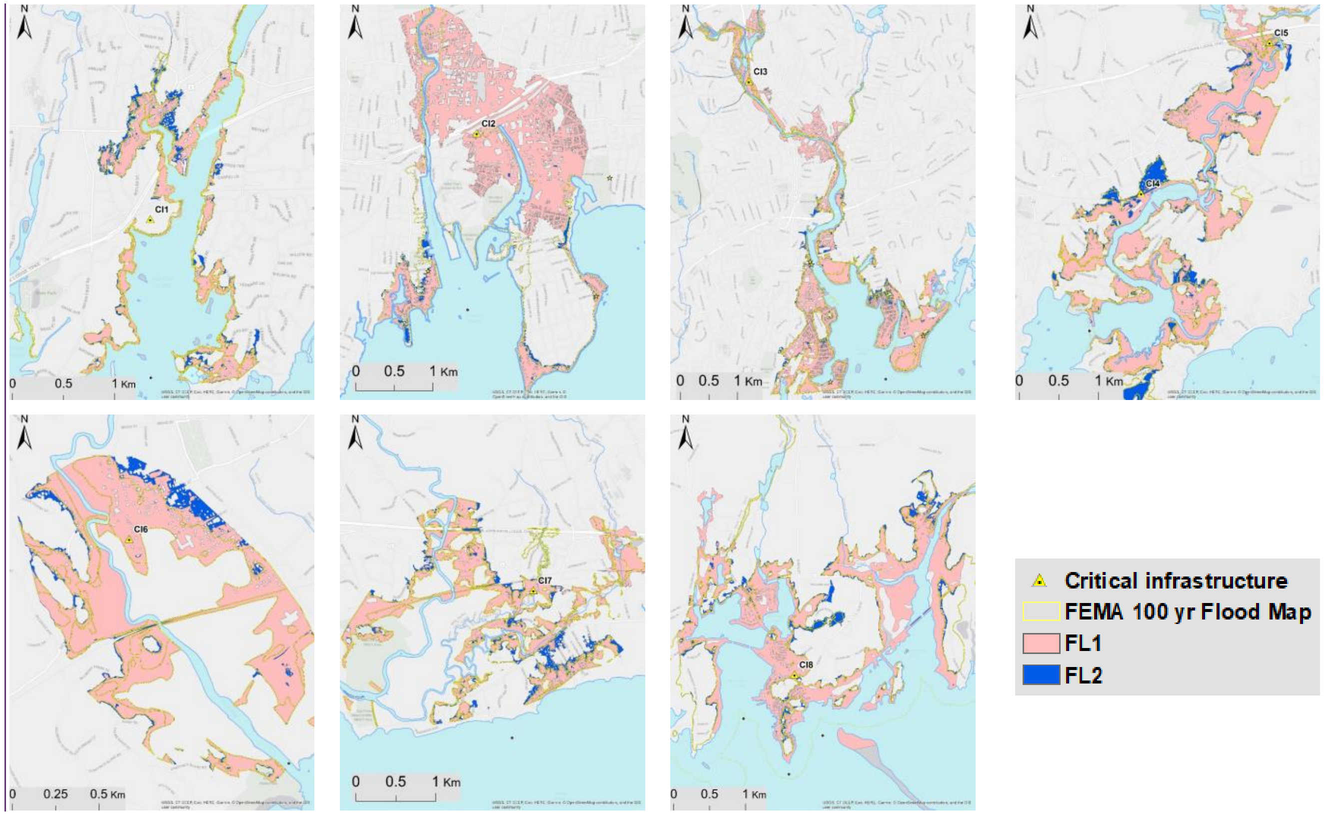

Figure 7c: Map overlay of maximum inundation for all the study domains containing CI1 through CI8 for the scenarios of Florence [FL1 and FL2, readers should refer to Table 3 and chapter 2.2 for specification on the scenarios]. Background map by ESRI web-services, provided by UConn/CTDEEP, Esri, Garmin, USGS, NGA, EPA, USDA, NPS

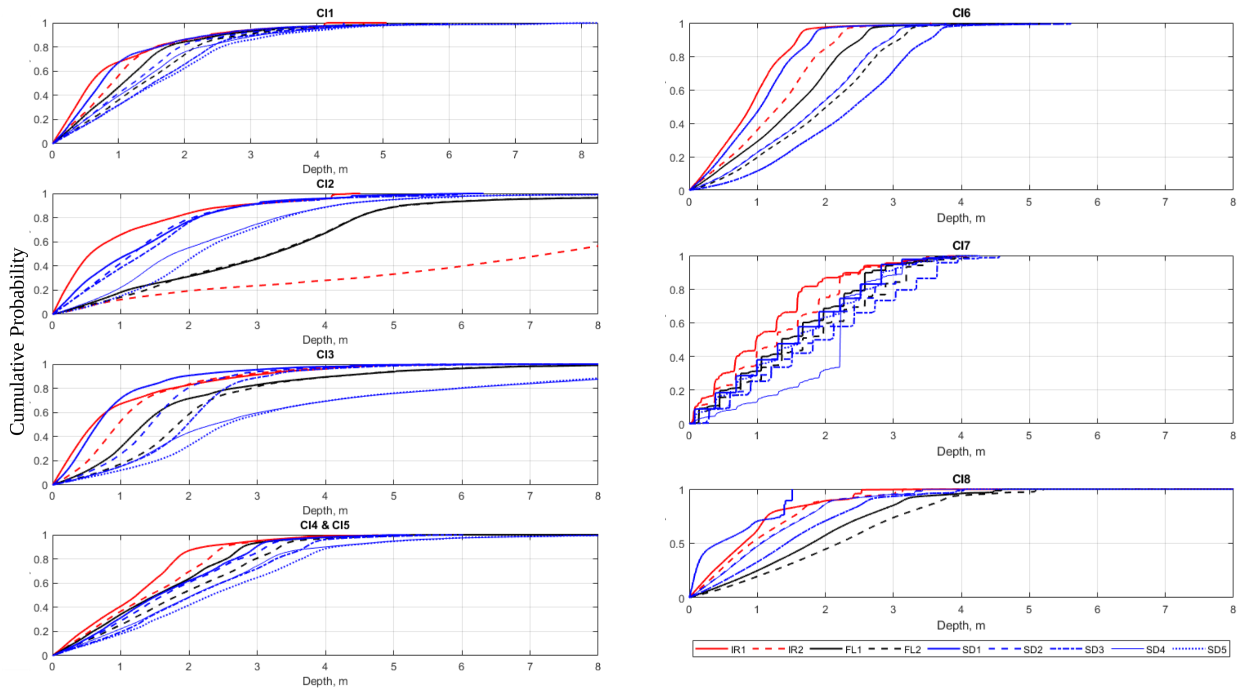

Figure 8: Cumulative density plot of the depth of all the flooded cells during maximum inundation. Hurricanes scenarios are labelled according to Table 3 and explained in chapter 2.2. Critical infrastructures are labelled CI1 to CI8, as described in Table 1.

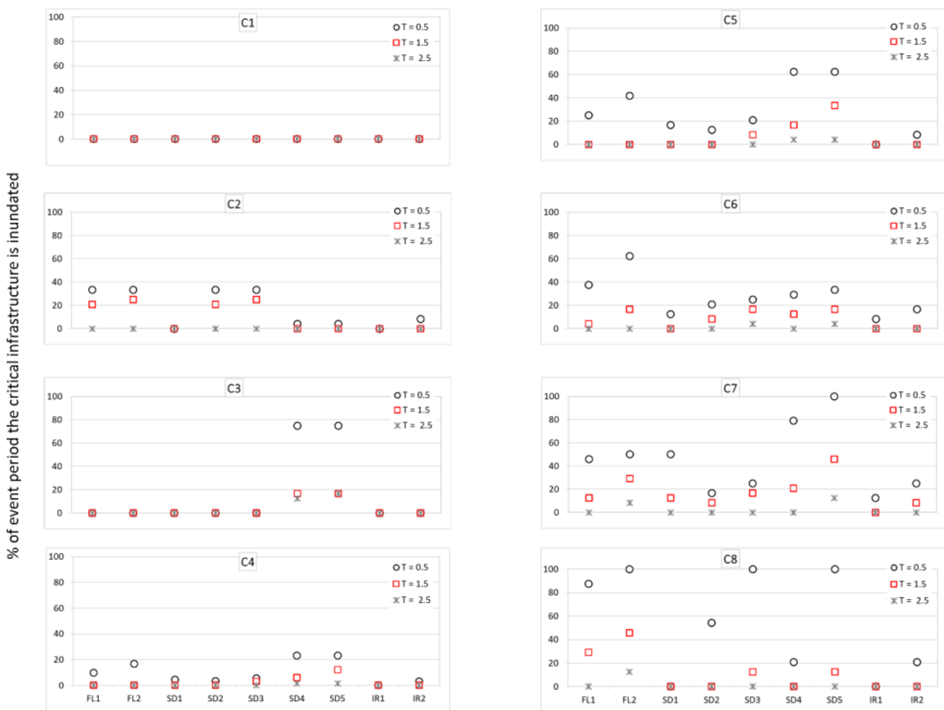

Figure ~~8~~9: Peak over threshold (T=0.5, 1.5 and 2.5m) at selected critical infrastructures. Hurricanes scenarios, along the x-axis, are ~~labelled~~labeled according to Table 3 and explained in chapter 2.2. Critical infrastructures are ~~labelled~~labeled CI1 to CI8, as described in Table 1.

Table 1: Study area- Characteristics of the considered CIs, with river and model domain information. Basin area represents the area of the underlining watershed; domain area is the extent of the simulation domain; reach length represents the length of the stream within the domain; hydrologic distance represents the distance from each CI to the coastline.

Critical Infrastructure (CI)	Town	Rivers	Basin area, km^2	Domain area, km^2	Reach length, km	Hydrologic ~~length~~distance, km
CI1	Coscob	Mianus River	216.6	7.5	7.8	4.5
CI2	Southend	Rippowam River	308.4	12.1	4.9	5.3
CI3	Norwalk	Norwalk River	268.7	20.7	8.3	7.8
CI4/ CI5	Branford	Branford River	84.5	7.9	6.7	8.8/5.3
CI6	Guilford	West River	126.4	2.2	3.7	5.1
CI7	Madison	East & Neck Rivers	173.0	8	5.3	6.8
CI8	Stonington	Stonington harbor	10.0	14.9	5.2	2.9

Table 2: Model domain information for Florence

Horizontal Resolution	18, 6, and 2 km
Vertical levels	28
Horizontal Grid Scheme	Arakawa C grid
Nesting	Two-way nesting
Convective parameterization	Grell 3D ensemble scheme (18 and 6 km grids only)
Microphysics option	Thompson graupel scheme (Thompson et al., 2008)
Longwave Radiation option	RRTM scheme (Mlawer et al., 1997)
Shortwave Radiation option	Goddard Shortwave scheme (Chou and Suarez 1994)
Surface-Layer option	Monin-Obukhov Similarity scheme
Land-Surface option	Noah Land-Surface Model (Tewari et al., 2004)
Planetary Boundary Layer	Yonsei scheme (Song–You et al., 2006)

Table 3:Table 3: Peak Tide, Surge at the maximum total water level instance, Accumulated precipitation & peak flows (with return period reported within brackets) for the simulated events. Recurrence interval (within brackets) and total volume of each event is also shown. Reader should refer to Chapter 2.2 for a detailed description of each hurricane scenario (IR for Irene, SD for Sandy, FL for Florence). Critical infrastructures are labelled CI1 to CI8 according to Table 1.

-	Accumulated precipitation (mm)				Peak flow, m^3/s (return period)			
CIs	IR1/IR2	SD1/SD2 /SD3	SD4/SD5	FL1/FL2	IR1/IR2	SD1/SD2 /SD3	SD4/SD5	FL1/FL2
CI1	187.8	24.8	555.3	128.5	158.5(56)	3.4(<2)	242.4(316)	51.3(<2)
CI2	177.8	24.7	546.9	147.5	201.1(58)	9.3(<2)	319.1(326)	87.4(5)
CI3	173.5	21.5	526.8	165.1	126.7 (26)	3.3 (<2)	201.7(28)	74.9(<2)
CI4/ CI5	98.1	17.0	338.2	192.0	93.9(5)	4.7(<2)	178.3(98)	106.1(13)
CI6	91.6	17.7	330.2	203.9	85.7(5)	1.3(<2)	168.4 (48)	113.3(8)
CI7	86.1	15.1	316.6	200.7	93.5(5)	0.9(<2)	197.0(301)	143.2(51)
CI8	58.5	8.9	323.7	289.2	30.8(3)	0.03(<2)	94.7(6)	93.1(6)

Table 4: Maximum total water levels (meter) for tide and surge at the downstream boundary.scenarios. Reader should refer to Chapter 2.2 for a detailed description of each hurricane scenario (IR for Irene, SD for Sandy, FL for Florence). The "*" denotes the scenarios having sea level rise (SLR) added to the surge. Critical infrastructures are labelled CI1 to CI8 according to Table 1.

Scenarios		CI1	CI2	CI3	CI4/ CI5	CI6	CI7	CI8
CIs FL1	FL2Tide (m)	SD10.99	SD2/ SD40 .99	SD3/ SD50 .99	IR10.94	IR20.94	0.94	0.17
	Surge (m)	2.51	2.51	2.51	2.56	2.46	2.56	3.33
	Accumulated precipitation (mm)	128.5	147.5	165.1	192	203.9	200.7	289.2
CI1	3.5Peak flow, m3/s (return period)	4.1 51.3 (<2.8)	3.8 87.4.4 (5)	74.9 (<2)	3106.1 (13)	113.3.7 (8)	143.2 (51)	93.1 (6)
FL2*	Tide (m)	0.99	0.99	0.99	0.94	0.94	0.94	0.17
CI2	Surge (m)	3.512	4.13.12	2.83.12	3.817	4.43.07	3.117	3.793
	Accumulated precipitation (mm)	128.5	147.5	165.1	192	203.9	200.7	289.2
CI3	Peak flow, m3/s (return period)	51.3.5 (<2)	87.4.1 (5)	74.9 (<2.8)	106.1 (13)	113.3.(8)	4.4 143.2.5 (51)	393.1 (6)
SD1	Tide (m)	0.82	0.82	0.82	0.4	0.4	0.4	0.01
CI4/ CI5	3.5Surge (m)	4.12.37	2.737	42.37	4.62.3	2.53	2.3.1	1.87

Deleted Cells
Inserted Cells
Inserted Cells
Deleted Cells
Deleted Cells
Inserted Cells
Inserted Cells
Inserted Cells
Inserted Cells
Deleted Cells
Inserted Cells
Inserted Cells
Inserted Cells

	Accumulated precipitation (mm)	24.8	24.7	21.5	17		17.7	15.1	8.9	
CI6	Peak flow, m3/s (return period)	3.4 (<2)	4.19.3 (<2)	3.3 (<2)	24.7 (<2)	4 4 2 - - 6 5	1.3.1 (<2)	0.9 (<2)	0.03 (<2)	
CI7SD2	3.5Tide (m)	4.1.01	2.1.01	3.1.01	3.71.13		2.51.13	3.1.13	-0.15	
	Surge (m)	2.56	2.56	2.56	2.8		2.8	2.8	1.95	
	Accumulated precipitation (mm)	24.8	24.7	21.5	17		17.7	15.1	8.9	
	Peak flow, m3/s (return period)	3.4 (<2)	9.3 (<2)	3.3 (<2)	4.7 (<2)		1.3 (<2)	0.9 (<2)	0.03 (<2)	
SD3*	Tide (m)	1.01	1.01	1.01	1.13		1.13	1.13	-0.15	
	Surge (m)	3.12	3.12	3.12	3.4		3.4	3.4	2.564016	
	Accumulated precipitation (mm)	24.8	24.7	21.5	17		17.7	15.1	8.9	
	Peak flow, m3/s (return period)	3.4 (<2)	9.3 (<2)	3.3 (<2)	4.7 (<2)		1.3 (<2)	0.9 (<2)	0.03 (<2)	
SD4	Tide (m)	1.01	1.01	1.01	1.13		1.13	1.13	-0.15	
	Surge (m)	2.56	2.56	2.56	2.8		2.8	2.8	1.95	
	Accumulated precipitation (mm)	555.3	546.9	526.8	338.2		330.2	316.6	323.7	
	Peak flow, m3/s (return period)	242.4 (316)	319.1 (326)	201.7 (28)	178.3 (98)		168.4 (48)	197.0 (301)	94.7 (6)	
SD5*	Tide (m)	1.01	1.01	1.01	1.13		1.13	1.13	-0.15	
	Surge (m)	3.12	3.12	3.12	3.4		3.4	3.4	2.564016	
	Accumulated precipitation (mm)	555.3	546.9	526.8	338.2		330.2	316.6	323.7	
	Peak flow, m3/s (return period)	242.4 (316)	319.1 (326)	201.7 (28)	178.3 (98)		168.4 (48)	197.0 (301)	94.7 (6)	
IR1	Tide (m)	1.16	1.16	1.16	1.1		1.1	1.1	0.93	
	Surge (m)	1.94	1.94	1.35	1.42		1.42	1.42	1.1	
	Accumulated precipitation (mm)	187.8	177.8	173.5	98.1		91.6	86.1	58.5	
CI8	Peak flow, m3/s (return period)	3158.5 (56)	4201.1 (58)	2.3126.7 (26)	293.9 (5)		85.7 (5)	393.5 (5)	1.430.8 (3)	2
IR2*	Tide (m)	1.16	1.16	1.16	1.1		1.1	1.1	2	
	Surge (m)	2.54	2.54	1.94	2.03		2.03	2.03	1.7	
	Accumulated precipitation (mm)	187.8	177.8	173.5	98.1		91.6	86.1	58.5	
	Peak flow, m3/s (return period)	158.5 (56)	201.1 (58)	126.7 (26)	93.9(5)		85.7 (5)	93.5 (5)	30.8 (3)	

Deleted Cells
Deleted Cells
Deleted Cells
Inserted Cells
Inserted Cells
Inserted Cells
Inserted Cells

Deleted Cells
Inserted Cells
Inserted Cells

Table 54: Overall extent of the inundated area (in km²), and the relative difference (% change in parenthesis) compared to the FEMA 100yr Flood Zone and dCorr (correlation between differences in flood extent as compared by FEMA, and flow and surge peak)

CIs	FL1	FL2	SD1	SD2	SD3	SD4	SD5	IR1	IR2	dCorr surge	dCorr flow
CI1	1.6 (-8.5)	1.8 (2.9)	0.9 (-48.1)	1.4 (-21.7)	1.9 (8.3)	1.7 (-2.8)	2.0 (13.9)	1.3 (-27.5)	1.5 (-15.9)	0.86	0.40
CI2	3.9 (134.2)	4.0 (139.4)	1.9 (-12.7)	2.1 (25.6)	2.3 (36.3)	3.7 (123.7)	4.8 (185.2)	1.6 (-1.9)	4.9 (192.2)	0.53	0.55
CI3	4.7 (2.6)	4.9 (7.5)	3.5 (-24.5)	4.0 (-10.5)	4.3 (-6.2)	5.4 (17.5)	7.1 (56.2)	3.2 (-29.3)	4.0 (-12.1)	0.67	0.70
CI4/CI5	2.7 (-8.3)	3.2 (8.4)	2.4 (-18.5)	2.6 (0.3)	3.4 (13.8)	2.9 (2.5)	3.6 (22.2)	2.0 (-32.3)	2.4 (-17.3)	0.98	0.43
CI6	0.9 (3.7)	0.9 (13.1)	0.7 (-14.9)	0.8 (-10.3)	1.0 (16.6)	0.9 (11.4)	1.0 (16.5)	0.7 (-20.4)	0.8 (-4.8)	0.84	0.56
CI7	2.5 (1.0)	2.7 (12.5)	1.6 (-33.9)	2.0 (-12.8)	2.6 (8.5)	2.1 (-10.7)	2.6 (7.3)	1.9 (-23.5)	2.3 (-7.5)	0.81	0.46
CI8	3.1 (4.5)	3.5 (18.4)	0.4 (-87.8)	2.1 (-28.8)	2.6 (-11.1)	2.2 (-22.3)	2.7 (-8.9)	1.1 (-63.1)	1.8 (-37.9)	0.88	0.67

Note: (-) Area inundated less than FEMA's 100yr zone

Inserted Cells

Inserted Cells